Small scale aspects of warm dark matter: Power spectra and acoustic oscillations

Daniel Boyanovsky and Jun Wu

Phys. Rev. D **83**, 043524 — Published 24 February 2011

DOI: 10.1103/PhysRevD.83.043524

Small scale aspects of warm dark matter : power spectra and acoustic oscillations.

Daniel Boyanovsky[1,*] and Jun Wu[1,†]

[1]*Department of Physics and Astronomy, University of Pittsburgh, Pittsburgh, PA 15260*

Abstract

We provide a semi-analytic derivation of approximate evolution equations for density perturbations of warm dark matter (WDM) candidates that decoupled while relativistic with arbitrary distribution functions, their solutions at small scales and a simple numerical implementation that yields their transfer functions and power spectra. Density perturbations evolve through three stages: radiation domination when the particle is relativistic and non-relativistic and matter domination. An early ISW effect during the first stage leads to an enhancement of density perturbations and a plateau in the transfer function for $k \lesssim k_{fs}$ the free streaming wave vector. An effective fluid description emerges at small scales which includes the effects of free streaming in initial conditions and inhomogeneities. The transfer function features *WDM-acoustic oscillations* at scales $k \gtrsim 2\,k_{fs}$. A simple analytic interpolation of the power spectra between large and small scales and a numerical implementation valid for arbitrary distribution functions is provided. As an application we study the power spectra for two models of sterile neutrinos with $m \sim$ keV produced non-resonantly and compare our results to those obtained from Boltzmann codes.

PACS numbers: 98.80.Cq; 98.80.-k; 98.80.Bp

*Electronic address: boyan@pitt.edu

†Electronic address: juw31@pitt.edu

I. INTRODUCTION

In the *concordance* ΛCDM standard cosmological model dark matter (DM) is composed of primordial particles which are cold and collisionless[1]. In this cold dark matter (CDM) scenario particles feature negligible small velocity dispersion leading to a power spectrum that favors small scales. Structure formation proceeds in a hierarchical "bottom up" approach: small scales become non-linear and collapse first and their merger and accretion leads to structure on larger scales, dense clumps that survive the merger process form satellite galaxies.

Large scale simulations seemingly yield an over-prediction of satellite galaxies[2] by almost an order of magnitude larger than the number of satellites that have been observed in Milky-Way sized galaxies[2–6]. Simulations within the ΛCDM paradigm also yield a density profile in virialized (DM) halos that increases monotonically towards the center[2, 7–10] and features a cusp, such as the Navarro-Frenk-White (NFW) profile[7] or more general central density profiles $\rho(r) \sim r^{-\beta}$ with $1 \leq \beta \lesssim 1.5$[4, 7, 10]. These density profiles accurately describe clusters of galaxies but there is an accumulating body of observational evidence[11–17, 19, 20] that suggest that the central regions of (DM)-dominated dwarf spheroidal satellite (dSphs) galaxies feature smooth cores instead of cusps as predicted by (CDM). This difference is known as the core-vs-cusp problem[17]. Salucci et.al.[18] reported that the mass distribution of spiral disk galaxies can be best fit by a cored Burkert-type profile.

In ref.[20] a "galaxy size" problem has been reported, where large scale simulations at $z = 3$ yield galaxies that are too small, this problem has been argued to be related to that of the missing dwarf galaxies.

Thus there seems to be emerging evidence that the ΛCDM paradigm for structure formation *may* have problems at small scales[21].

Warm dark matter (WDM) particles were invoked[22–24] as possible solutions to the discrepancies both in the over abundance of satellite galaxies and as a mechanism to smooth out the cusped density profiles predicted by (CDM) simulations into the cored profiles that fit the observations in (dShps). (WDM) particles feature a range of velocity dispersion in between the (CDM) and hot dark matter leading to free streaming scales that smooth out small scale features[25] and could be consistent with core radii of the (dSphs). If the free streaming scale of these particles is smaller than the scale of galaxy clusters, their large scale

structure properties are indistinguishable from (CDM) but may affect the *small* scale power spectrum[26] so as to provide an explanation of the smoother inner profiles of (dSphs), fewer satellites and the size of galaxies at $z = 3$[20].

Furthermore recent numerical results hint to more evidence of possible small scale discrepancies with the ΛCDM scenario: another over-abundance problem, the "emptiness of voids" [27] and the spectrum of "mini-voids"[28] both may be explained by a WDM candidate. Constraints from the luminosity function of Milky Way satellites[29] suggest a lower limit of $\sim 1\,\mathrm{keV}$ for a WDM particle, a result consistent with Lyman-α[30–32], galaxy power spectrum[33] and lensing observations[34]. More recently, results from the Millenium-II simulation[35] suggest that the ΛCDM scenario *overpredicts* the abundance of massive $\gtrsim 10^{10}\,M_\odot$ haloes, which is corrected with a WDM candidate of $m \sim 1\,\mathrm{keV}$. This body of emerging evidence in favor of WDM as possible solutions to these potential small scale problems of the ΛCDM scenario warrants deeper understanding of their small scale clustering properties.

A model independent analysis suggests that dark matter particles with a mass in the keV range is a suitable (WDM) candidate[36, 37], and sterile neutrinos with masses in the $\sim$ keV range are compelling (WDM) candidates[38–51]. These neutrinos can decay into an active-like neutrino and an X-ray photon[52], and recent astrophysical evidence in favor of a 5 keV line has been presented in ref.[53] (see also[54]). The analysis in ref.[55] suggests upper mass limits for a sterile neutrino in the range $\sim 6 - 10$ keV. Possible *direct* detection signals of such candidates have been recently assessed in ref.[56].

A property of a dark matter candidate relevant for structure formation is its distribution function after decoupling[57, 59–61]. It depends on the production mechanism and the (quantum) kinetics of its evolution from production to decoupling. There are different production mechanisms of sterile neutrinos[38–41, 43–51, 57, 58, 62], leading in general to non-thermal distribution functions. There is some tension between the X-ray[52] and Lyman-α forest[30–32] data if sterile neutrinos are produced via the Dodelson-Widrow (DW)[38] non-resonant mixing mechanism, leading to the suggestion[55] that these may not be the dominant (DM) component. Constraints from the Lyman-α forest spectra are particularly important because of its sensitivity to the suppression of the power spectrum by free-streaming in the linear regime[30–32]. The gravitational clustering properties of collisionless (DM) in the linear regime are described by the power spectrum of gravitational perturba-

tions. Free streaming of collisionless (DM) leads to a suppression of the transfer function on length scales smaller than the free streaming scale via Landau damping[26, 63, 64]. This scale is determined by the decoupling temperature, the particle's mass and the distribution function at decoupling[65].

Goals: The most accurate manner to obtain the transfer function for DM perturbations is to use the publicly available computer codes for cosmic microwave background (CMB) anisotropies[66–68], with modifications that would allow to include the different distribution functions of the WDM particles. These codes include baryons, radiation, neutrinos and DM and yield very accurate numerical results. The drawbacks in using these codes for WDM particles are that they do not readily yield to an understanding of what aspects of a distribution function influence the small scale behavior, and must be modified for the individual WDM candidates because their distribution functions are "hard-wired" in the codes.

The goals of this article are twofold:

- **i):** a semi-analytic derivation and solution of the evolution equations for (WDM) density perturbations, understanding of the main physical processes that determine the transfer function of WDM candidates at *small scales that entered the horizon well before matter-radiation equality* for *arbitrary* distribution functions.

- **ii):** to provide a relatively simple formulation of the power spectrum that allows a straightforward and efficient numerical implementation, valid for arbitrary distribution functions.

In order to achieve these goals we must necessarily invoke several approximations: a) we neglect the contribution from baryons, b) we also neglect anisotropic stresses resulting from the free streaming of ultrarelativistic standard model *active* neutrinos. These approximations entail that the results of the transfer functions will be trustworthy up to $10-15\%$ accuracy. However, the main purpose of this work is *not* to obtain the WDM transfer function to a few percent accuracy, but to provide a semi-analytic "tool", to study the main features of the transfer function *at small scales* for a particular WDM candidate given its distribution function determined by the microscopic process of production and decoupling. If the transfer function features important small scale properties that could potentially lead

to substantial changes in structure formation, this would warrant more accurate study with the CMB codes and eventual inclusion into N-body simulations.

In this article we study the transfer function for WDM density and gravitational perturbations by solving the collisionless Boltzmann equation in a *radiation and matter* dominated cosmology including the perturbations from the radiation fluid for arbitrary distribution function of the WDM particle, thus the results (within the acknowledged possible errors) are valid for $z > 2$.

Strategy:

WDM particles with a mass in the $\sim$ keV range typically decouple from the primordial plasma when they are still relativistic in the radiation dominated era and become non-relativistic when $T \approx m \approx$ keV when the size of the comoving horizon $\eta \lesssim$ Mpc.

Therefore we anticipate *three stages* of evolution for density perturbations: I) when the particle is still relativistic, this is a radiation dominated (RD) stage, II) when the particle is non-relativistic but still during the (RD) era, III) when matter perturbations dominate the gravitational potential (the particle is non-relativistic in this era). When the WDM particles are relativistic, their contribution to the total radiation component is negligible because their effective number of degrees of freedom is $\ll 1$ (see below). Therefore during stages I) and II) the gravitational potential is completely determined by the radiation fluid. Our strategy is to solve the Boltzmann equation for WDM density perturbations in the three stages. In stages I) and II) the gravitational potential is completely determined by the radiation fluid and the Boltzmann equation is solved by considering the gravitational potential as a *background* determined by the Einstein-Boltzmann equation for the radiation fluid. In stage III) when matter perturbations dominate, the 00-Einstein equation for small scale perturbations is equivalent to Poisson's equation. The initial conditions for the Boltzmann equation are given deep in the (RD) era when the relevant modes are well outside the horizon. In this work we consider adiabatic initial conditions determined by the primordial perturbations seeded during inflation. The main strategy is to use the solution of the integration of the Boltzmann equation in a previous stage as the *initial condition* for the next stage. During stage I) suppression by free streaming is independent of the distribution function and the free streaming scale grows with the comoving horizon. However we find that modes that enter the horizon when the particle is relativistic with wavelengths up to the sound horizon

are amplified via an early integrated Sachs-Wolfe effect (ISW) as a consequence of the time dependence of the gravitational potential produced by acoustic oscillations of the radiation fluid. The evolution of WDM density perturbations at the end of this stage determine the initial conditions for stage II) when the particle becomes non-relativistic but still the gravitational potential is determined by the perturbations in the radiation fluid. During this stage the free streaming scale depends only logarithmically on the comoving horizon. Whereas CDM perturbations grow logarithmically during this stage (Meszaros effect), WDM perturbations are suppressed by a free streaming function that depends on the distribution function of the decoupled WDM particle. In stage III) when WDM perturbations dominate the gravitational potential, density perturbations obey a self-consistent Boltzmann-Poisson integral equation which we analyze in a systematic expansion valid for small scales.

The main results are:

- The main results are a semi-analytic derivation of the evolution for density perturbations of WDM species that decoupled during radiation domination with adiabatic superhorizon initial conditions. A solution of the evolution equations throughout the three states, and a simple numerical implementation that yields the WDM transfer function and power spectrum for arbitrary distribution functions.

- During the (RD) era acoustic oscillations in the radiation fluid determine the gravitational potential ϕ. The time dependence of ϕ induces an early ISW that results in an *enhancement* of the amplitude of WDM density perturbations for wavelengths larger than the sound horizon of the radiation fluid at η_{NR} when the particle becomes non-relativistic.

- In stage III), we turn the Boltzmann-Poisson equation into a self-consistent differential integral equation that admits a systematic Fredholm series solution. Its leading term is the Born approximation and lends itself to a simple and straightforward numerical analysis for arbitrary distribution functions. This approximation is equivalent to a fluid description *but with an inhomogeneity and initial conditions completely determined by the past history during stages I) and II)*. The resulting fluid equation is a WDM generalization of Meszaros equation[69–71]. The solutions describe *WDM acoustic oscillations*, the suppression by free streaming is manifest in the inhomogeneity and initial conditions.

- In the Born approximation we obtain a semi-analytic expression for the transfer function and compare it to the CDM case. We also provide an expression for the power spectra that interpolates between large and small scales and give a concise summary for its numerical evaluation for arbitrary distribution functions, mass and decoupling temperature.

- Although we do *not* advocate nor endorse any particular WDM model, as an application of the method and illustration of the results we study in detail the transfer functions and power spectra of sterile neutrinos with $m \sim$ keV. There are many different suitable mechanisms for sterile neutrino production[38–41, 43–51, 57, 58, 62] and as specific examples in this article we focus on two different scenarios of sterile neutrinos produced non-resonantly: via the (DW) mechanism[38] and via boson decay[43, 57, 58]. Although we recognize that Lyman- α constraints[30–32, 55] may already rule out the (DW) mechanism, we nevertheless study this case because we can compare the results from our semi-analytic method to the results of Boltzmann codes obtained in refs.[32, 41, 42] for this particular case, thereby establishing a solid benchmark for the reliability of results found here. The second choice, provides a microscopic distribution function obtained from a quantum kinetic description which also describes the production of sterile neutrinos by inflaton[43] and gravitino[62] decay. Whereas the (DW) distribution function departs from thermality *only* in an overall constant $\beta \ll 1$ that multiplies the Fermi-Dirac distribution function, in the (BD) case the distribution function resulting from freeze out at temperatures of the order of the electroweak scale is highly non-thermal with an enhancement at low momentum which reduces the velocity dispersion, this non-thermality and the higher decoupling temperature effectively make this species colder than (DW). Thus the first choice provides a benchmark test case for comparison with results available in the literature[32, 41, 42]. The results of the Born approximation agree to $< 5\%$ with the numerical fit to the transfer function provided in ref.[32] in the region where the fit is valid. The second choice provides a definite contrast to the (DW) case that allows us to glean how details of the distribution function affect the transfer function and power spectra at small scales.

This work differs from that in ref.[72] that analyzes (standard model active) neutrinos as

(WDM) but in an Einstein-Desitter cosmology, in two main aspects: i) our study includes the (RD) era and the transition to matter domination (MD) including the time dependence of the gravitational potential, which is a source of an early ISW effect during stage I) and the history during stages I) and II), and ii) we study non-thermal distribution functions. The inclusion of stages I) and II) during the (RD) era also distinguishes this work from that in ref.[57, 61].

II. PRELIMINARIES

We consider a radiation and matter dominated cosmology:

$$H^2 = \frac{\dot{a}^2}{a^4} = H_0^2 \left[\frac{\Omega_r}{a^4} + \frac{\Omega_m}{a^3} \right] = \frac{H_0^2 \Omega_m}{a^4} \left[a + a_{eq} \right] \tag{II.1}$$

where the dot stands for derivative with respect to conformal time (η), the scale factor is normalized to $a_0 = 1$ today, and

$$a_{eq} = \frac{\Omega_r}{\Omega_m} \simeq \frac{1}{3229} \,. \tag{II.2}$$

Introducing

$$\tilde{a} = \frac{a}{a_{eq}} \,, \tag{II.3}$$

it follows that

$$\frac{d\,\tilde{a}}{d\eta} = \left[\frac{H_0^2 \Omega_m}{a_{eq}} \right]^{\frac{1}{2}} \left[1 + \tilde{a} \right]^{\frac{1}{2}} \tag{II.4}$$

leading to

$$\eta = \frac{2}{\left[\frac{H_0^2 \Omega_m}{a_{eq}} \right]^{\frac{1}{2}}} \left[\sqrt{1+\tilde{a}} - 1 \right] \equiv 288.46 \left[\sqrt{1+\tilde{a}} - 1 \right] (\mathrm{Mpc}) \,, \tag{II.5}$$

where we have used $\Omega_m h^2 = 0.134$[73]. At matter-radiation equality we define

$$k_{eq} \equiv H_{eq}\, a_{eq} = \sqrt{2} \left[\frac{H_0^2 \Omega_m}{a_{eq}} \right]^{\frac{1}{2}} = \frac{9.8 \times 10^{-3}}{\mathrm{Mpc}} \tag{II.6}$$

corresponding to the comoving wavevector that enters the Hubble radius at matter-radiation equality. Furthermore from (II.5) we find the comoving size of the horizon at matter-radiation equality,

$$\eta_{eq} = \frac{2\sqrt{2}(\sqrt{2}-1)}{H_{eq} a_{eq}} \simeq \frac{1.172}{H_{eq} a_{eq}} \simeq 120\,\mathrm{Mpc} \tag{II.7}$$

from which we obtain

$$\tilde{a} = \frac{\eta}{\eta^*}\left[1 + \frac{\eta}{4\eta^*}\right] \quad ; \quad \eta^* = \frac{\eta_{eq}}{2(\sqrt{2}-1)} = \frac{\sqrt{2}}{k_{eq}}\,. \tag{II.8}$$

During radiation domination

$$\tilde{a} \approx \left(\frac{\eta}{\eta^*}\right) \ll 1\,, \tag{II.9}$$

and in this regime

$$\eta \simeq \tilde{a}\ 144.23\ (\text{Mpc})\,. \tag{II.10}$$

During matter-radiation domination, a comoving wavevector k enters the (comoving) Hubble radius when $k = Ha$ corresponding to a value of the scale factor

$$\tilde{a}_k = \frac{1 + \sqrt{1 + 8\left(\frac{k}{k_{eq}}\right)^2}}{4\left(\frac{k}{k_{eq}}\right)^2}\,. \tag{II.11}$$

We are interested in small scale properties for perturbations with comoving wavelenghts $100\,\text{pc} \leq \lambda \equiv 2\pi/k < 10\,\text{Mpc}$ corresponding to $k \gg k_{eq}$. For these modes, which have entered the horizon during the radiation dominated era, it follows that

$$\tilde{a}_k \sim \sqrt{2}\ \frac{k_{eq}}{k} \ll 1\,. \tag{II.12}$$

A weakly interacting massive particle (WIMP) of mass $m \sim 100$ GeV that undergoes chemical freeze-out at $T_{ch} \sim m/20$ and thermal decoupling at $T_d \sim 10$ MeV when $\tilde{a}_d \sim 10^{-7}$, and $\eta_d \sim 10$ pc, i.e, deep in the (RD) era, is non-relativistic at decoupling. Scales $\lesssim \eta_d$ where inside the horizon when the DM particle was still coupled to the cosmological plasma and acoustic oscillations of the photon fluid are imprinted on the transfer function at these very small scales[74]. However, larger scales were outside the horizon and their perturbations are frozen, they enter the horizon after decoupling and their evolution is described by the collisionless Boltzmann equation.

On the other hand, sterile neutrinos with mass $m \sim$ keV decoupled thermally at much higher temperature (~ 150 MeV for (DW)[38], ~ 100 GeV for production via scalar or vector boson decay[57, 58]), and become non-relativistic at $T \sim m \sim$ keV, namely for $\tilde{a} \sim 10^{-3}$. In terms of conformal time, $m \sim$ keV sterile neutrinos become non-relativistic at

$$\eta_{NR} \sim 0.2\ \text{Mpc}\left(\frac{\text{keV}}{m}\right), \tag{II.13}$$

so that for $\eta \ll \eta_{NR}$ this (DM) candidate is relativistic and non-relativistic for $\eta > \eta_{NR}$. Therefore, for DM candidates that decoupled for temperatures $T_d \gtrsim 10\,\mathrm{MeV}$ all modes of cosmological relevance for (comoving) scales $\lambda \gtrsim 50\,\mathrm{pc}$ may be studied in the linear regime via the collisionless Boltzmann-Vlasov equation. A firmer estimate will be provided in section (III A).

For WDM particles with $m \sim$ keV we see from eqns. (II.12, II.6) that comoving scales $\lambda \gtrsim 0.2\,\mathrm{Mpc}$ entered the horizon when the DM particle is non-relativistic, whereas smaller scales entered during the radiation dominated stage when the WDM particle is *relativistic*. Therefore comoving scales smaller than that of cluster of galaxies became sub-horizon during (RD) when the WDM particle is still *relativistic*. This is important because free streaming changes from the relativistic to the non-relativistic case: during the relativistic stage the free streaming length is of the order of the horizon, but much smaller during the non-relativistic stage (see below).

Hence as anticipated above, there are three distinct stages of evolution of density perturbations for WDM particles with $m \sim$ keV and scales smaller than $0.2 - 1\,\mathrm{Mpc}$:

- **I**) (RD), relativistic $\eta < \eta_{NR}$,
- **II**) (RD), non-relativistic $\eta_{eq} > \eta > \eta_{NR}$,
- **III**) matter domination (MD), non-relativistic for $\eta \geq \eta_{eq}$.

III. EVOLUTION OF PERTURBATIONS: THE BOLTZMANN EQUATION

We follow the notation of Ma and Bertschinger[75] (see also[76–80]), and consider only scalar perturbations in the conformal Newtonian gauge (longitudinal gauge) with a perturbed metric

$$g_{00} = -a^2(\eta)\Big[1 + 2\psi(\vec{x},\eta)\Big] \tag{III.1}$$

$$g_{ij} = a^2(\eta)\Big[1 - 2\phi(\vec{x},\eta)\Big]\,\delta_{ij}\,. \tag{III.2}$$

The perturbed distribution function is given by

$$f(p,\vec{x},\eta) = f_0(p) + F_1(p,\vec{x},\eta) \tag{III.3}$$

where $f_0(p)$ is the unperturbed distribution function, which after decoupling obeys the collisionless Boltzmann equation in absence of perturbations and $\vec{p}, \vec{x}$ are comoving momentum and coordinates respectively. As discussed in ref.[57, 60, 61] the unperturbed distribution function is of the form

$$f_0(p) \equiv f_0(y; x_1, x_2, \cdots) \tag{III.4}$$

where

$$y = \frac{p}{T_{0,d}} \tag{III.5}$$

where p is the comoving momentum and $T_{0,d}$ is the decoupling temperature *today*,

$$T_{0,d} = \Big(\frac{2}{g_d}\Big)^{\frac{1}{3}}\, T_{CMB}\,, \tag{III.6}$$

with g_d being the effective number of relativistic degrees of freedom at decoupling, $T_{CMB} = 2.35 \times 10^{-4}$ eV is the temperature of the (CMB) today, and x_i are dimensionless couplings or ratios of mass scales.

The methods and main results presented below are general and valid for arbitrary f_0. However, although we do not endorse or advocate any particular WDM model it is obviously important to test the results of our semi-analytic study and the reliability of the numerical implementation and to provide at least some preliminary understanding of the influence of the details of the distribution function on the WDM power spectrum within some established models, here we focus our discussion on sterile neutrinos with the mass range $m \sim$ keV. These candidates may be produced by many different mechanisms[38–41, 43–51, 57, 58] as mentioned above.

While we do not advocate or endorse a production mechanism, in this article we apply the results and numerical implementation to analyze in detail two test scenarios: sterile neutrinos produced by the Dodelson-Widrow (DW) (non-resonant) mechanism for which

$$f_0(p) = \frac{\beta}{e^y + 1} \tag{III.7}$$

where $\beta \simeq 10^{-2}$[38], and sterile neutrinos produced by the decay of a scalar with a mass of the order of the EW scale or vector bosons (BD), which are abundant at temperatures near the EW scale[57, 58],

$$f_0(p) = \lambda\, \frac{g_{5/2}(y)}{\sqrt{y}} \quad ; \quad g_{5/2}(y) = \sum_{n=1}^{\infty} \frac{e^{-n\,y}}{n^{\frac{5}{2}}} \tag{III.8}$$

and $\lambda \sim 10^{-2}$[57, 58]. This distribution function is similar to that found from inflaton[43] and gravitino[62] decays.

As discussed above, (DW) sterile neutrinos may already be ruled out by observations, however we study this model because it allows us to directly compare our results with the power spectrum obtained with Boltzmann codes in refs.[32, 41, 42] thereby establishing a benchmark for the semi-analytic method and its numerical implementation. The (BD) case represents a highly non-thermal distribution function obtained in different scenarios and provides a clear contrast with the (DW) case allowing to glean how the small scale aspects of the power spectra depend on the distribution function. A next step in the program will apply the method to the study of the power spectra for other WDM candidates.

We will also compare the results for the WDM distributions with that for weakly interacting massive particles (WIMPs) which freeze-out with a Maxwell-Boltzmann (MB) distribution,

$$f_0(p) = \mathcal{N}\ e^{-\frac{y^2}{2x}} \quad ; \quad x = \frac{m}{T_d} \tag{III.9}$$

where $m \sim 100$ GeV, $T_d \sim 10$ MeV is the thermal decoupling temperature, and $\mathcal{N}$ is determined at chemical freeze-out[82].

An important observation for WDM candidates is that during the radiation dominated era when these are relativistic, their contribution to the energy density is

$$\rho = \frac{1}{a^4}\int \frac{d^3p}{(2\pi)^3}\ p\, f_0(p) \propto T^4(t) \times \begin{cases} \beta & \text{(DW)} \\ \lambda & \text{(BD)} \end{cases} \tag{III.10}$$

for sterile neutrinos produced by the Dodelson-Widrow (DW) or scalar decay (BD) mechanisms. Namely these WDM candidates contribute to the radiation component with an effective number of degrees of freedom proportional to $\beta, \lambda, \sim 10^{-2}$ and *can be safely neglected in their contribution to the radiation component*. The same argument justifies neglecting the anisotropic stress (quadrupole moment) arising from the free streaming of these particles when they are relativistic.

Introducing spatial Fourier transforms in terms of comoving momenta $\vec{k}$ (we keep the same notation for the spatial Fourier transform of perturbations), the linearized Boltzmann equation for perturbations is given by[75–80]

$$\dot{F}_1(\vec{k},\vec{p};\eta) + i\frac{k\,\mu\,p}{\epsilon(p,\eta)}\;F_1(\vec{k},\vec{p};\eta) + \Big(\frac{d\;f_0(p)}{dp}\Big)\Big[p\;\dot{\phi}(\vec{k},\eta) - ik\,\mu\,\epsilon(p,\eta)\;\psi(\vec{k},\eta)\Big] = 0 \quad \text{(III.11)}$$

where $\mu = \widehat{\mathbf{k}}\cdot\widehat{\mathbf{p}}$, dots stand for derivative with respect to conformal time η and

$$\epsilon(p,\eta) = \sqrt{p^2 + m^2\,a^2(\eta)} \quad \text{(III.12)}$$

is the conformal energy of the particle of mass m. During (RD) and (MD), the 00 component of Einstein's equation in conformal Newtonian gauge is[76]

$$\phi(\vec{k},\eta) + 3\frac{\mathcal{H}}{k}\left(\frac{1}{k}\,\dot{\phi}(\vec{k},\eta) + \frac{\mathcal{H}}{k}\psi(\vec{k},\eta)\right) = -\frac{3}{4}\frac{k_{eq}^2}{k^2\,\tilde{a}^2}\left[\tilde{a}\left(\frac{\delta\rho}{\rho}\right)_m + \left(\frac{\delta\rho}{\rho}\right)_r\right], \quad \text{(III.13)}$$

where

$$\mathcal{H} = \frac{\dot{\tilde{a}}}{\tilde{a}} = aH = k_{eq}\,\frac{[1+\tilde{a}]^{\frac{1}{2}}}{\sqrt{2}\,\tilde{a}} \quad \text{(III.14)}$$

is the inverse comoving Hubble radius, and

$$\delta\rho_j(\vec{k},\eta) = \frac{1}{a^4}\;\int\frac{d^3p}{(2\pi)^3}\;\epsilon(p,\eta)\;F_{1,j}(\vec{k},\vec{p},\eta)\;\;;\;\;j = r,m\,. \quad \text{(III.15)}$$

In what follows we neglect stress anisotropies leading to

$$\phi(\vec{k},\eta) = \psi(\vec{k},\eta)\,, \quad \text{(III.16)}$$

thereby neglecting the quadrupole moment from relativistic standard model (active) neutrinos. We also neglect the baryonic component in the matter contribution, a compromise that allows us to pursue a semi-analytic understanding of the (DM) transfer function at small scales. The remaining Einstein's equations are not necessary for the discussion that follows. In absence of stress anisotropy, Einstein's equation (III.13) can be written in another useful form,

$$\frac{2}{3}\frac{k^2\tilde{a}^2}{k_{eq}^2}\,\phi + (1+\tilde{a})\Big(\tilde{a}\,\phi\Big)' = -\frac{1}{2}\left[\tilde{a}\left(\frac{\delta\rho}{\rho}\right)_m + \left(\frac{\delta\rho}{\rho}\right)_r\right] \quad \text{(III.17)}$$

where

$$' \equiv \frac{d}{d\tilde{a}}\,. \quad \text{(III.18)}$$

The formal solution of the Boltzmann equation (III.11) is

$$F_1(\vec{k},\vec{p};\eta) = F_1(\vec{k},\vec{p};\eta_i)\;e^{-ik\,\mu\,l(p,\eta,\eta_i)} - p\left(\frac{d\,f_0(p)}{dp}\right)\;\int_{\eta_i}^{\eta} d\tau\;e^{-ik\,\mu\,l(p,\eta,\tau)}\left[\frac{d\phi(\vec{k},\tau)}{d\tau} - i\;\frac{k\,\mu}{V(p,\tau)}\;\phi(\vec{k},\tau)\right] \quad \text{(III.19)}$$

where

$$l(p,\eta,\eta') = \int_{\eta'}^{\eta} V(p,\tau)\ d\tau \quad ; \quad V(p,\tau) = \frac{p}{\epsilon(p,\tau)} \tag{III.20}$$

is the comoving *free streaming* distance that a particle travels between η' and η with *physical* velocity $V(p,\tau) = p/\epsilon(p,\tau)$.

The solution (III.19) with (III.20) is the starting point of our analysis. The density and gravitational perturbations produced by a WDM particle with $m \sim$ keV that decouples from the plasma when it is still relativistic are obtained by evolving the solution (III.19) through the three stages : I) when the DM particle is still relativistic during (RD), II) when the particle becomes non-relativistic for $\tilde{a} \gtrsim 10^{-3}$ but still during (RD), III) during (MD) $\tilde{a} \geq 1$ (the DM particle is non-relativistic).

During the first two stages the perturbation in the gravitational potential ϕ in (III.19) is completely determined by the radiation component to which the WDM candidate contributes negligibly as discussed above. The difference between stages I) and II) is manifest in the free streaming distance $l(p,\eta,\eta')$. During stage III) the gravitational potential is determined by the DM density perturbations self-consistently through Poisson's equation (this is the advantage of the conformal Newtonian gauge). Our strategy is to determine initial conditions deep in the radiation era when the cosmologically relevant modes are still superhorizon, and to evolve the solution (III.19) through each of these stages, using the distribution function at the end of each stage as the initial condition for the next stage, thereby propagating the initial condition determined deep in the radiation era to matter-radiation equality.

A. Free streaming distance:

The free streaming distance $l(p,\eta,\eta')$ can be obtained analytically with (II.8), the general result can be expressed in terms of elliptic functions, however it is unyielding and not very illuminating. It simplifies considerably in two relevant cases: for radiation domination when $\eta \ll \eta_{eq}$ which includes the era when the DM candidate becomes non-relativistic, and in the non-relativistic regime for $\eta \gg \eta_{NR}$ which includes the matter dominated era.

Radiation domination (RD):

Since $f_0(p)$ is a function of $y = p/T_{0,d}$ it is convenient to write $p = yT_{0,d}$ in $V(p)$. In the

radiation dominated era $\eta \ll \eta_{eq}$ during which $a(\eta) \sim \eta/\eta^*$ we find

$$k\, l(p,\eta,\eta') = \frac{\alpha\, y}{2}\, \ln\left[\frac{z + \sqrt{\frac{y^2\alpha^2}{4} + z^2}}{z' + \sqrt{\frac{y^2\alpha^2}{4} + z'^{\,2}}}\right] \;\; ; \;\; z = k\eta \tag{III.21}$$

where we have introduced

$$\alpha = 2\sqrt{2}\, \frac{k\, T_{0,d}}{m\, k_{eq} a_{eq}} \simeq 2.15 \times 10^{-3} \left(\frac{k}{k_{eq}}\right) \left(\frac{2}{g_d}\right)^{\frac{1}{3}} \left(\frac{\rm keV}{m}\right) \simeq 0.22\, k \left(\frac{2}{g_d}\right)^{\frac{1}{3}} \left(\frac{\rm keV}{m}\right) \times \left({\rm Mpc}\right). \tag{III.22}$$

Since for the WDM distributions under consideration $y^2 f(y)$ is strongly peaked at $y \sim \sqrt{\overline{y^2}}$ where

$$\overline{y^2} = \frac{\int_0^\infty y^4 f_0(y) dy}{\int_0^\infty y^2 f_0(y) dy} = \begin{cases} \frac{105}{12}\, \frac{\zeta(7)}{\zeta(5)} \simeq 8.505 \; ; \;\; \text{for (BD)} \\ \\ 15\, \frac{\zeta(5)}{\zeta(3)} \simeq 12.939 \; ; \; \text{for (DW } \textit{or} \text{ thermal fermion)} \\ \\ 3\, x = 3\, \frac{m}{T_d} \; ; \qquad \text{for (MB)} \end{cases} \tag{III.23}$$

it follows that for $z, z' \ll \sqrt{\overline{y^2}}\, \alpha$ the ultrarelativistic approximation $v(p,\eta) \sim 1$ is valid[1], and in this regime

$$l(p,\eta,\eta') = (\eta - \eta')\,, \tag{III.24}$$

which is the comoving free streaming distance traveled by an ultrarelativistic particle between η and η'. In the opposite limit when the particle is non-relativistic but still in the radiation dominated era $z, z' \gg \sqrt{\overline{y^2}}\, \alpha$ it follows that

$$k\, l(p,\eta,\eta') = \alpha\, \frac{y}{2}\, \ln\left[\frac{z}{z'}\right]. \tag{III.25}$$

Non-relativistic WDM

From the expression of the conformal energy (III.12) and the physical velocity $V(p,\tau)$ in (III.20) we see that the particle is relativistic if $p \gg m\, a(\eta)$ and non-relativistic for $p \ll m\, a(\eta)$. Since the comoving momentum is integrated over and weighted by the distribution function, we define

$$\tilde{a}_{NR} = \frac{\langle p^2 \rangle^{\frac{1}{2}}}{m\, a_{eq}}\,, \tag{III.26}$$

[1] The condition $z \ll \sqrt{\overline{y^2}}\, \alpha$ is equivalent to $\langle p^2 \rangle \gg m^2 a^2(\eta)$, where the average is with $f_0(p)$.

where the average is taken with the distribution $f_0(p)$ as the value of $\tilde{a}$ that determines the transition between the relativistic and non-relativistic regime, the particle is relativistic for $\tilde{a} \ll \tilde{a}_{NR}$ and non-relativistic for $\tilde{a} > \tilde{a}_{NR}$. When the particle is non-relativistic

$$V(p,\eta) = \frac{p}{m\,a(\eta)}\,. \tag{III.27}$$

therefore

$$\tilde{a}_{NR} = \langle V^2(t_{eq})\rangle^{\frac{1}{2}}\,. \tag{III.28}$$

Writing $p = y\,T_{0,d}$ we find

$$\langle V^2(t_{eq})\rangle^{\frac{1}{2}} \simeq 7.59\ \times 10^{-4}\,\sqrt{\overline{y^2}}\left(\frac{\mathrm{keV}}{m}\right)\left(\frac{2}{g_d}\right)^{\frac{1}{3}}. \tag{III.29}$$

A weakly interacting massive particle (WIMP) (CDM) of mass $\sim 100\,\mathrm{GeV}$ and $T_d \sim 10\,\mathrm{MeV}$ features $\langle V^2(t_{eq})\rangle^{\frac{1}{2}} \simeq 4\ \times 10^{-8}$, whereas for a WDM candidate with $m \sim$ keV we find $\langle V^2(t_{eq})\rangle^{\frac{1}{2}} \lesssim 10^{-3}$, namely all these DM candidates are non-relativistic at t_{eq} with $\langle V^2(t_{eq})\rangle \ll 1$. Since the WDM particle is non-relativistic at the epoch of matter-radiation equality $\tilde{a}_{NR} \ll 1$, we find from eqns. (II.8,II.10) that

$$\eta_{NR} = \frac{\sqrt{2}}{k_{eq}}\,\langle V^2(t_{eq})\rangle^{\frac{1}{2}}\,, \tag{III.30}$$

for $\eta \gg \eta_{NR}$ the particle is non-relativistic and relativistic for $\eta \ll \eta_{NR}$.

Since in the non-relativistic stage the physical velocity is given by (III.27), the integral in (III.20) is easily performed by changing integration variable from $\eta \to \tilde{a}$, we find

$$k\,l(p,\eta,\eta') = y\,\alpha\,[u - u']\,, \tag{III.31}$$

where we introduced

$$u(\eta) = \frac{1}{2}\,\ln\left[\frac{\sqrt{1+\tilde{a}(\eta)}-1}{\sqrt{1+\tilde{a}(\eta)}+1}\right] = \frac{1}{2}\,\ln\left[\frac{\eta}{4\eta^* + \eta}\right]\ \ ;\ \ u_{NR} \leq u(\eta) \leq 0\,, \tag{III.32}$$

where $\tilde{a}_{NR} = \tilde{a}(\eta_{NR})$, normalized $u(\eta)$ so that $u(\infty) = 0$ and introduced

$$u_{NR} = \ln\left[\frac{\sqrt{\tilde{a}_{NR}}}{2}\right]. \tag{III.33}$$

During the radiation era when the WDM particle is non-relativistic, $\tilde{a} \ll 1$ we find that

$$k\,l(p,\eta,\eta') = \frac{\alpha\,y}{2}\,\ln\left[\frac{\eta}{\eta'}\right] \tag{III.34}$$

which reproduces the result (III.25). During the matter dominated era for $\tilde{a} \gg 1$ it follows that

$$u(\eta) \sim -\frac{1}{\sqrt{\tilde{a}(\eta)}} \sim -\frac{2\eta^*}{\eta}\,. \tag{III.35}$$

Free-streaming wavevector from fluid analogy

In analogy with the Jean's wavevector in the fluid description of perturbations during matter domination, we introduce the *comoving* free-streaming wavevector

$$k_{fs}^2(t) = \frac{4\pi G\rho_m(t)}{\langle \vec{V}^2(t)\rangle}\, a^2(t) \tag{III.36}$$

where

$$\rho_m(t) = \frac{\rho_m(0)}{a^3(t)} \;\;;\;\; \langle \vec{V}^2(t)\rangle = \frac{\langle \vec{V}^2(0)\rangle}{a^2(t)} \tag{III.37}$$

and the value of the velocity dispersion *today* is

$$\langle \vec{V}^2(0)\rangle = \overline{y^2}\left(\frac{T_{d,0}}{m}\right)^2. \tag{III.38}$$

We note that

$$k_{fs}(a_{eq}) \equiv \frac{2\pi}{\lambda_{fs}} = \frac{\sqrt{3}}{2}\,\frac{k_{eq}}{\langle \vec{V}^2(t_{eq})\rangle^{\frac{1}{2}}}\,, \tag{III.39}$$

Therefore for these particles

$$k_{fs}(a_{eq}) \gg k_{eq}\,. \tag{III.40}$$

We *define* the free streaming wavevector as

$$k_{fs} \equiv k_{fs}(a_{eq}) = \frac{11.17}{\sqrt{\overline{y^2}}}\left(\frac{m}{\mathrm{keV}}\right)\left(\frac{g_d}{2}\right)^{\frac{1}{3}}(\mathrm{Mpc})^{-1}\,. \tag{III.41}$$

This scale will be seen to play a fundamental role in the (DM) transfer function.

For a $m \sim$ keV sterile neutrino produced non-resonantly by boson decay (BD) that decoupled near the electroweak scale[57] ($g_d \sim 100$), it follows that

$$k_{fs}^{BD} \sim 14.12\,(\mathrm{Mpc})^{-1}\,, \tag{III.42}$$

whereas for a similar mass sterile neutrino produced non-resonantly via the (DW) mechanism near the QCD scale ($g_d \sim 30$) we find

$$k_{fs}^{DW} \sim 7.7\,(\mathrm{Mpc})^{-1}\,. \tag{III.43}$$

and for a WIMP of $m \sim 10\,\mathrm{GeV}$ that decoupled thermally at $T_d \sim 10\,\mathrm{MeV}$ one finds $k_{fs} \sim 10^6\,(\mathrm{Mpc})^{-1}$. We will see later that k_{fs} determines the scale of suppression of the transfer function.

It is convenient to introduce

$$\kappa \equiv \sqrt{\overline{y^2}}\,\alpha \equiv \frac{\sqrt{6}\,k}{k_{fs}} = \sqrt{6}\,\frac{\lambda_{fs}}{\lambda} = 2\,\sqrt{2}\,\frac{k}{k_{eq}}\,\langle \vec{V}^2(t_{eq})\rangle^{\frac{1}{2}}\,. \tag{III.44}$$

where $\overline{y^2}$ is given by (III.23) for the DM species considered here, and $\lambda_{fs} = 2\pi/k_{fs}$. The dimensionless ratio κ will be important in the discussion of non-relativistic DM.

From (III.31,III.32) we find

$$k\,l(p,\eta_0,\eta_{eq}) \simeq y\alpha \ln\left[\sqrt{2}+1\right] \tag{III.45}$$

where η_0 is the conformal time *today*, namely $l(p,\eta_0,\eta_{eq})$ is the free streaming distance traveled by the non-relativistic WDM particle from matter-radiation equality until today. Combining this result with eqn. (III.39) we find[2]

$$l(p,\eta_0,\eta_{eq}) \simeq 0.344\,\frac{y}{\sqrt{\overline{y^2}}}\,\lambda_{fs}\,. \tag{III.46}$$

From which it follows that during matter domination λ_{fs}, which is the equivalent of the Jeans length for *collisionless* matter perturbations, is simply related to the free streaming distance traveled by the non-relativistic particle moving with average comoving momentum $\sqrt{\langle p^2\rangle}$ from the time of matter-radiation equality until today, namely $\lambda_{fs} \approx 2.9\; l\big(\sqrt{\langle p^2\rangle},\eta_0,\eta_{eq}\big)$.

From (III.29) and (III.33) we find

$$u_{NR} \simeq -4.27 + \frac{1}{2}\ln\left[\frac{\sqrt{\overline{y^2}}}{3}\left(\frac{\mathrm{keV}}{m}\right)\left(\frac{50}{g_d}\right)^{\frac{1}{3}}\right], \tag{III.47}$$

where the argument of the logarithm is $\mathcal{O}(1)$ for $m \sim$ keV sterile neutrinos produced via the (DW) or (BD) mechanisms.

From eqns. (II.8,III.30) we find the relation

$$\eta_{NR} = \frac{\sqrt{2}}{k_{eq}}\,\langle \vec{V}^2(t_{eq})\rangle^{\frac{1}{2}} = \frac{\sqrt{3}}{\sqrt{2}\,k_{fs}}\,, \tag{III.48}$$

[2] The slight discrepancy with the result in ref.[61] can be traced back to the difference between matter only and matter-radiation evolution.

hence from the definition of κ, eqn. (III.44) and (III.30) it follows that

$$k\,\eta_{NR} = \frac{\kappa}{2}\,. \tag{III.49}$$

Therefore comoving modes that entered the horizon when the particle is still relativistic correspond to $\kappa \gtrsim 2 \Rightarrow k \gtrsim k_{fs}$ whereas those that entered when the particle is non-relativistic correspond to $\kappa \lesssim 2 \Rightarrow k \lesssim k_{fs}$. The main corollary is that the free streaming wavelength is *of the order of the size of the horizon at the time when the (DM) particle transitions from being relativistic to non-relativistic.*

This is important: when the particle is relativistic the free streaming distance grows with the comoving horizon η and free streaming is most efficient to erase density perturbations, whereas when the particle is non-relativistic, the free streaming distance grows only with the logarithm of the comoving horizon and free streaming is less efficient to erase perturbations because the particle free streams with a small velocity. Therefore the dimensionless ratio κ indicates the regimes in which free streaming is more ($\kappa \gg 2$) or less ($\kappa \ll 2$) efficient to suppress density perturbations.

B. Initial conditions

Initial conditions are determined deep in the radiation dominated era and when the wavelengths are well outside the horizon. We will only consider adiabatic initial conditions for which *all* the radiation components feature the same $\delta\rho_r/\rho_r$ and (non-relativistic) matter perturbations obey

$$\left(\frac{\delta\rho}{\rho}\right)_m = \frac{3}{4}\left(\frac{\delta\rho}{\rho}\right)_r\,. \tag{III.50}$$

For the radiation component temperature perturbations correspond to a perturbation in the distribution function

$$F_{1,r}(\vec{k},\vec{p};\eta_i) = -\Theta(\vec{k},\eta_i)\,p\Big(\frac{df_{0,r}(p)}{dp}\Big) \quad ; \quad \Theta(\vec{k},\eta_i) = \frac{\Delta T(\vec{k},\eta_i)}{T_0} \tag{III.51}$$

so that

$$\left(\frac{\delta\rho}{\rho}\right)_{i,r} = 4\Theta(\vec{k},\eta_i)\,. \tag{III.52}$$

For superhorizon perturbations when perturbations in the radiation component are nearly constant the temperature anisotropy is determined by the Newtonian potential[75–77]

$$\Theta(\vec{k},\eta_i) = -\frac{1}{2}\,\phi_i(k) \quad ; k\,\eta_i \ll 1\,. \tag{III.53}$$

Initial conditions for adiabatic perturbations of the *matter* component *also* correspond to

$$F_{1,m}(\vec{k},\vec{p};\eta_i) = -\Theta(\vec{k},\eta_i)\, p\Big(\frac{df_{0,m}(p)}{dp}\Big) \tag{III.54}$$

which leads to

$$\frac{\delta\rho_m(\vec{k},\eta_i)}{\rho_m} = -\Theta(\vec{k},\eta_i)\ \frac{\int p^3\left(\frac{df_{0,m}(p)}{dp}\right)dp}{\int p^2\, f_{0,m}(p)\, dp} = 3\,\Theta(\vec{k},\eta_i) = \frac{3}{4}\left(\frac{\delta\rho}{\rho}\right)_{i,r} \tag{III.55}$$

The subtlety for WDM candidates is that in setting up initial conditions for superhorizon fluctuations, small comoving scales are superhorizon when the WDM candidate is *relativistic* and intermediate and large comoving scales are superhorizon when the particle has become non-relativistic. However, adiabatic initial conditions for *all* modes are determined by (III.54). Indeed, when the WDM candidate is relativistic such initial condition yields an energy density perturbation which is adiabatic for a radiation component and when the particle is non-relativistic it gives the corresponding relation (III.50). Therefore adiabatic initial conditions for all modes (superhorizon at the initial time η_i) for the WDM perturbations are

$$F_1(\vec{k},\vec{p};\eta_i) = \frac{1}{2}\,\phi_i(k)\, p\left(\frac{df_0(p)}{dp}\right)\ \ ;\ \ k\,\eta_i \ll 1\,, \tag{III.56}$$

where $f_0(p)$ is the unperturbed distribution function for the DM candidate, and $\phi_i(k)$ is the primordial gravitational potential determined during inflation.

In what follows it is convenient to *define*

$$\widetilde{F}(\vec{k},\vec{p};\eta) = \frac{F_1(\vec{k},\vec{p};\eta)}{n_0}\ \ ;\ \ \widetilde{f}(p) = \frac{f_0(p)}{n_0} \tag{III.57}$$

where

$$n_0 = \int \frac{d^3p}{(2\pi)^3}\, f_0(p)\,, \tag{III.58}$$

is the density of (DM) *today*. Furthermore, we introduce

$$\delta(\vec{k},\eta) = \int \frac{d^3p}{(2\pi)^3}\, \widetilde{F}(\vec{k},\eta)\,. \tag{III.59}$$

which becomes $\delta\rho_m/\rho_m$ after the DM particle becomes non-relativistic, its initial condition is

$$\delta_i(k) \equiv \delta(\vec{k},\eta_i) = -\frac{3}{2}\phi_i(k)\ \ ;\ \ \text{for } k\eta_i \ll 1\,. \tag{III.60}$$

C. Long wavelength perturbations:

We begin by studying the evolution of $\phi(k,\eta)$ for long-wavelength modes that remain superhorizon throughout, to establish the normalization of the transfer function.

For $k \to 0$ the solution of the Boltzmann equation (III.19) becomes the *same* for DM or radiation (relativistic) components namely

$$\widetilde{F}(\eta) = \widetilde{F}(\eta_i) - \left(p\frac{d\widetilde{f}}{dp}\right)[\phi(\eta) - \phi(\eta_i)] \,, \tag{III.61}$$

where we have suppressed the argument $\vec{k}$ since we consider only $k = 0$ here.

For the radiation component we write, following eqn. (IV.2)

$$\widetilde{F}_r(\eta) = -\Theta(\eta)\left(p\frac{d\widetilde{f}}{dp}\right) \tag{III.62}$$

leading to the solution

$$\Theta(\eta) = \phi(\eta) - \frac{3}{2}\phi_i \tag{III.63}$$

where we used the initial condition (III.53). For DM perturbations, from eqn. (III.59) we obtain

$$\delta(\eta) = 3\phi(\eta) - \frac{9}{2}\phi_i \tag{III.64}$$

where we used the initial condition (III.60).

For a DM particle that decouples while relativistic and during the stage when it is still relativistic $\delta\rho/\rho \neq \delta$. However, for a WDM particle with $m \sim$ keV it follows that $\delta\rho/\rho = \delta$ for $\tilde{a} \gtrsim \tilde{a}_{NR} \sim 10^{-3}$. Hence, for $\tilde{a} \gtrsim \tilde{a}_{NR}$ the Einstein equation (III.17) becomes

$$\frac{2}{3}\frac{k^2\tilde{a}^2}{k_{eq}^2}\,\phi + (1+\tilde{a})\left[\tilde{a}\,\phi^{'} + \phi\right] = -\frac{1}{2}\left[\tilde{a}\,\delta + 4\Theta\right] \tag{III.65}$$

where we have used (III.14). Using the solutions of the Boltzmann equations (III.63,III.64) for $k = 0$, and defining $\widetilde{\phi} = \phi/\phi_i$, we find

$$\widetilde{\phi}' + \widetilde{\phi}\left[\frac{5\,\tilde{a}+6}{2\,\tilde{a}\,(1+\tilde{a})}\right] = \frac{3}{4\tilde{a}}\left[\frac{3\,\tilde{a}+4}{1+\tilde{a}}\right] \tag{III.66}$$

the solution of this equation is

$$\widetilde{\phi}(\tilde{a}) = \frac{\sqrt{1+\tilde{a}}}{\tilde{a}^3}\int_0^{\tilde{a}}\frac{3}{4y}\left[\frac{3\,y+4}{1+y}\right]\frac{y^3\,dy}{\sqrt{1+y}} + \mathcal{C}\left[\frac{\sqrt{1+\tilde{a}}}{\tilde{a}^3}\right] \,, \tag{III.67}$$

and $\mathcal{C}$ is determined by giving $\widetilde{\phi}(\tilde{a}_{NR})$. Since $\tilde{a}_{NR} \leq 10^{-3}$ for the DM candidates studied here, we will take $\tilde{a}_{NR} \to 0$ whence $\widetilde{\phi}(\tilde{a}_{NR} \to 0) = 1$, namely we are assuming that the DM particle becomes non-relativistic when the Newtonian potential still has the primordial superhorizon value. With this initial condition we find

$$\widetilde{\phi}(\tilde{a}) = \frac{1}{10\,\tilde{a}^3}\left[16\sqrt{1+\tilde{a}} + 9\tilde{a}^3 + 2\tilde{a}^2 - 8\tilde{a} - 16\right], \tag{III.68}$$

a result that agrees with those found in refs.[76, 81]. For $\tilde{a} \ll 1$ it follows that $\widetilde{\phi}(\tilde{a}) = 1 - \tilde{a}/10 + \mathcal{O}(\tilde{a}^2)$ therefore the approximation $\phi(\tilde{a}_{NR}) \simeq \phi(0) = \phi_i$ is very reliable. $\widetilde{\phi}(\tilde{a})$ decreases monotonically from $\widetilde{\phi}(0) = 1$ to $\widetilde{\phi}(\infty) = 9/10$, and at matter-radiation equality $\widetilde{\phi}(1) = 0.963$.

For $k \neq 0$ the transfer function for the Newtonian potential is *defined* as

$$\tilde{\phi}(k; \tilde{a} \gg 1) \equiv \frac{9}{10}\, T(k) \;\; ; \;\; T(0) = 1\,. \tag{III.69}$$

Whereas long wavelength perturbations in the gravitational potential remain nearly constant, short wavelength perturbations fall off as a consequence of suppression by free streaming.

For $k\tilde{a} \gg k_{eq}$ the first term in the left hand side of Einstein's equation (III.17) dominates, leading to Poisson's equation

$$\phi(k, \tilde{a}) = -\frac{3}{4}\frac{k_{eq}^2}{k^2\tilde{a}^2}\left[\tilde{a}\left(\frac{\delta\rho}{\rho}\right)_m + \left(\frac{\delta\rho}{\rho}\right)_r\right]. \tag{III.70}$$

IV. EVOLUTION OF DENSITY PERTURBATION DURING RADIATION DOMINATION.

Although the Newtonian potential is determined by Einstein's equation (III.13) where the right hand side also has a contribution from the DM perturbations during the stage when they are relativistic, such contribution is negligible because of the perturbatively small effective number of degrees of freedom ($\beta, \lambda \sim 10^{-2}$) as discussed above.

Hence, during the (RD) era $\tilde{a} \ll 1$ the DM perturbations can be neglected, and the evolution of the perturbations is completely determined by the evolution of the radiation fluid. In this case there is an exact solution for the Newtonian potential[76–81]

$$\phi(z) = -3\,\phi_i(k)\left[\frac{\left(\frac{z}{\sqrt{3}}\right)\,\cos(\frac{z}{\sqrt{3}}) - \sin(\frac{z}{\sqrt{3}})}{(\frac{z}{\sqrt{3}})^3}\right] \;\; ; \;\; z = k\,\eta \tag{IV.1}$$

where ϕ_i the primordial value of the Newtonian potential determined during inflation. The solution (IV.1) reflects the acoustic oscillations of the radiation fluid with speed of sound $c_s = 1/\sqrt{3}$.

A. Relativistic DM: stage I

During the(RD) stage in which the DM particle is still relativistic, namely for $k\eta \ll \sqrt{\overline{y^2}}\,\alpha$ the free streaming distance $l(p,\eta,\eta') = \eta - \eta'$ and $v(p,\eta) = 1$, the integrand in (III.19) does not depend on p. In this case it proves convenient to write

$$\widetilde{F}(\vec{k},\vec{p}\;\eta) = -\Theta(k,\mu;\,\eta)\,p\,\Big(\frac{d\widetilde{f}(p)}{dp}\Big)\,, \tag{IV.2}$$

and we find

$$\Theta(k,\mu;\,\eta) = -\phi(z) + e^{-i\mu\,z}\left[\frac{1}{2}\,\phi_i(k) + 2\int_0^z dz'\Big(\frac{d\phi(z')}{dz'}\Big)\,e^{i\mu\,z'}\right] \;\;;\;\; z = k\,\eta\,. \tag{IV.3}$$

Expanding $\Theta(k,\mu;\,\eta)$ in Legendre polynomials,

$$\Theta(k,\mu;\,\eta) = \sum_{l=0}^{\infty}(-i)^l\,(2l+1)\,\Theta_l(k;\,\eta)\mathcal{P}_l(\mu) \tag{IV.4}$$

we obtain

$$\Theta_l(k;\,\eta) = -\phi(z)\,\delta_{l,0} + \frac{1}{2}\,\phi_i(k)\,j_l(z) + 2\int_0^z dz'\Big(\frac{d\phi(z')}{dz'}\Big)j_l(z-z')\,, \tag{IV.5}$$

where we have taken $k\,\eta_i = 0$. The last term describes an ISW contribution akin to that in the temperature perturbations of photons[76]. We note that if the mode remains outside the horizon all throughout the evolution during the (RD) stage in which the DM particle is relativistic, namely $k\,\eta = z \ll 1$, it follows that

$$\Theta_l(z) = -\frac{1}{2}\,\phi_i(k)\,\delta_{l,0} + \mathcal{O}(z)\,. \tag{IV.6}$$

The WDM density perturbation

$$\delta(k;\,\eta) = \frac{1}{2}\int_{-1}^{1} d\mu\,\int_0^\infty \widetilde{F}(\vec{k},\vec{p};\,\eta)\frac{p^2dp}{4\pi^2}\,, \tag{IV.7}$$

therefore during the RD era when the DM perturbation is relativistic

$$\delta(k;\eta) = 3\,\Theta_0(z) \;\;;\;\; \delta(k;\,\eta_i) = -\frac{3}{2}\,\phi_i(k)\,. \tag{IV.8}$$

The monopole $\Theta_0(z)$ begins to grow when it enters the horizon as a consequence of the ISW contribution, it reaches a maximun and damps out as a consequence of (relativistic) free streaming. This is understood from the following argument: at early time the derivative of the Newtonian potential is negative and its modulus increases, reaching a maximum approximately at the sound horizon $k\eta \simeq \sqrt{3}\,\pi$, whereas the free streaming function $j_0(z-s)$ is approximately constant for $z \sim s$, therefore the integrand receives the largest contribution near the upper limit, and the total integral peaks near the sound horizon. However, at later times the integrand is strongly suppressed by free-streaming since $d\phi/ds$ peaks near the sound horizon, but for $z \gg \pi\sqrt{3}$ the free-streaming function suppresses the integrand. Fig. (1) displays $\Theta_0(z)/\Theta_0(0)$.

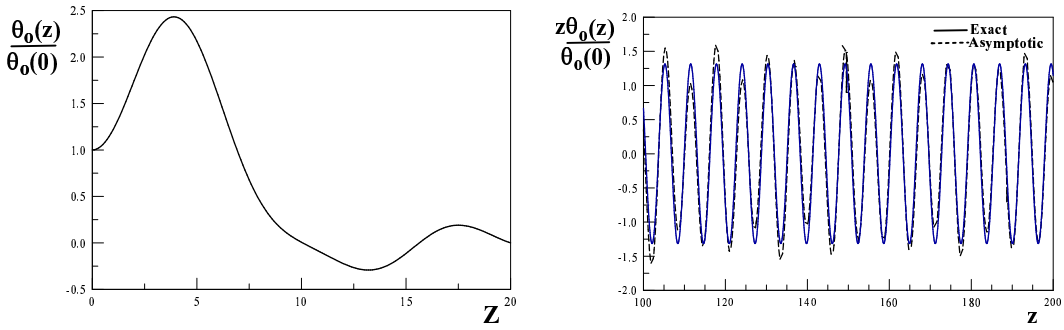

FIG. 1: Left panel $\frac{\Theta_0(z)}{\Theta_0(0)}$, right panel: $z\Theta_0(z)/\Theta_0(0)$ compared to the asymptotic form (IV.10) for the monopole.

Although an analytic expression for the integrals in (IV.5) is not readily available, we can obtain a reliable asymptotic expansion for $z \gg 1$. For this purpose it is convenient to integrate by parts the derivative of the Newtonian potential, for $z \gg 1$ the contributions near the upper limit of the integral $s \sim z$ vanish rapidly and the integral is dominated by the small s region since the Newtonian potential $\propto 1/s^2$ for large s. Using the asymptotic expansion

$$j_l(z) = \frac{\sin(z - \frac{l\pi}{2})}{z} + \mathcal{O}\big(\frac{1}{z^3}\big) \tag{IV.9}$$

and setting $z \to \infty$ in the upper limit of the integrals we find for $z \gg 1$

$$\Theta_l(z) \stackrel{z\gg 1}{=} 3\phi_i(k)\,\frac{\sin\left[z - \frac{l\pi}{2}\right]}{z}\left[\frac{5}{2} - \sqrt{3}\,\ln\left(\frac{\sqrt{3}+1}{\sqrt{3}-1}\right)\right] + \mathcal{O}\left(\frac{1}{z^2}\right), \tag{IV.10}$$

this damped oscillatory behavior emerges for $z \gtrsim 15$.

We note that the oscillations in (IV.10) do not feature the frequency corresponding to sound waves, the only remnant of the acoustic oscillations of the radiation fluid in the asymptotic form is in the terms featuring the $\sqrt{3}$ in the prefactor of the asymptotic form (IV.10).

An important conclusion of this section is that during the stage in which the DM particle is *relativistic* density perturbations *do not depend* on the unperturbed distribution function and particle statistics.

When the particle becomes non-relativistic, for modes $k\,\eta_{NR} \gg 1$ the asymptotic form is still valid, and the monopole features oscillatory behavior

$$\Theta_0(k) \propto \frac{\sin\frac{\kappa}{2}}{\kappa}\,. \tag{IV.11}$$

This oscillatory behavior is a consequence of the acoustic oscillations of the radiation fluid, numerically we find that oscillations arise for $\kappa/2 \gtrsim 15$ (see fig. (1)).

B. Non-relativistic DM: stages II and III

When the DM particle becomes non-relativistic (NR) $\epsilon(p,\eta) \sim m\,a(\eta)$; $v(p,\eta) = p/m\,a(\eta)$. It proves convenient to change from η to a new variable s defined by

$$ds = \frac{d\eta}{a(\eta)} \Rightarrow s(\eta) = \frac{2\,u(\eta)}{\left[H_0^2\,\Omega_m a_{eq}\right]^{\frac{1}{2}}} = \frac{2\sqrt{2}\,u}{k_{eq}a_{eq}} \tag{IV.12}$$

where $u(\eta)$ is given by eqn. (III.32). The solution of the Boltzmann equation for the normalized perturbation (III.57) is

$$\begin{aligned}\widetilde{F}(\vec{k},\vec{p};s) \;=\; & -\phi(\vec{k},s)\left(p\,\frac{d\widetilde{f}}{dp}\right) + \int_{s_{NR}}^{s} ds'\left\{ima^2(s')\,\phi(\vec{k},s')\left(\vec{k}\cdot\vec{\nabla}_p\widetilde{f}\right)\left[1+\frac{p^2}{m^2\,a^2(s')}\right]\right\} e^{-i\frac{\vec{k}\cdot\vec{p}}{m}(s-s')} \\ & +\; e^{-i\frac{\vec{k}\cdot\vec{p}}{m}(s-s_{NR})}\left[\widetilde{F}(\vec{k},\vec{p};\eta_{NR}) + \phi(\vec{k},\eta_{NR})\left(p\,\frac{d\widetilde{f}}{dp}\right)\right].\end{aligned} \tag{IV.13}$$

The initial "time" $s_{NR} = s(\eta_{NR})$ corresponds to the (conformal) time at which the DM particle becomes non-relativistic. For WIMP's that decoupled thermally for $T_d \ll m$ at conformal time $\eta_d \sim 10$ pc during the (RD) era, s_{NR} can be taken to be $s_{NR} = s(\eta_d)$. Modes with comoving scales much larger than η_d where outside the horizon at s_{NR}, for these modes the initial condition is given by eqn. (III.56), namely

$$\widetilde{F}(\vec{k},\vec{p};\eta_{NR}) = \frac{1}{2}\,\phi_i(k)\,p\left(\frac{d\widetilde{f}(p)}{dp}\right). \tag{IV.14}$$

On the other hand, WDM particles with $m \sim$ keV WDM decouple when they are still relativistic, namely $T_d \gg m$. For these candidates comoving scales that enter the horizon during the (RD) stage when the WDM particle is still relativistic evolve until the particle becomes non-relativistic at $\eta = \eta_{NR}$ as described in the previous section. Therefore $s_{NR} = s(\eta_{NR})$ and

$$\widetilde{F}(\vec{k}, \vec{p};\, \eta_{NR}) = -\Theta(k, \mu;\, \eta_{NR})\, p \left(\frac{d\widetilde{f}(p)}{dp}\right), \tag{IV.15}$$

where $\Theta(k, \mu;\, \eta_{NR})$ is given by equations (IV.4,IV.5) with $\eta = \eta_{NR}$. Integrating eqn. (IV.13) by parts in s' and $\vec{p}$, and neglecting the term $(p/m\, a(s))^2 \ll 1$ in the non-relativistic limit, the evolution of the density perturbation is given by

$$\begin{aligned}\tilde{\delta}(\vec{k}, s) \;=\; & 3\phi(k, s) - k^2 \int_{s_{NR}}^{s} ds' a^2(s') \phi(k, s')\, (s - s')\, K(k, s - s') \\ & + \int \frac{d^3p}{(2\pi)^3}\, p \left(\frac{d\widetilde{f}(p)}{dp}\right) e^{-i\frac{\vec{k}\cdot\vec{p}}{m}(s - s_{NR})}\; \mathcal{S}\big[\vec{k}, \vec{p}; \eta_{NR}\big]\,. \end{aligned} \tag{IV.16}$$

where

$$K(k, s - s') = \int \frac{d^3p}{(2\pi)^3}\, e^{-i\frac{\vec{k}\cdot\vec{p}}{m}(s - s')}\, \widetilde{f}(p) \tag{IV.17}$$

determines the suppression by non-relativistic free streaming and

$$\mathcal{S}\big[\vec{k}, \vec{p}; \eta_{NR}\big] = \frac{3}{2}\phi_i(k) e^{-i\mu z_{NR}} + 2\, i\mu \int_0^{z_{NR}} dz' \phi(z')\, e^{-i\mu(z_{NR} - z')} \quad ; \quad z = k\eta \tag{IV.18}$$

is the result of evolution during stage I and determines the initial condition for the evolution during the non-relativistic stages II and III.

Since f_0 only depends on p, using eqns. (IV.12,III.22) it follows that

$$K(k, s - s') \equiv K[\alpha(u - u')] = \frac{1}{N} \int y^2 f_0(y) j_0[y\alpha(u - u')]\, dy \quad ; \quad N = \int y^2 f_0(y)\, dy \tag{IV.19}$$

and j_0 is the spherical Bessel function.

The first line in (IV.16) integrates the gravitational potential during the stages in which the particle is non-relativistic. As described above, there are two distinct epochs: when the gravitational potential is dominated by perturbations in the radiation fluid and when it is dominated by dark matter perturbations. The crossover between the two stages occurs at a scale $s^* \equiv s(a^*)$ that is determined self-consistently, for $s > s^*$ the matter perturbation dominates the gravitational potential.

It is convenient to separate the contributions to the gravitational potential from the DM and radiation components, writing in obvious notation $\phi(k, \eta) = \phi_r(k, \eta) + \phi_m(k, \eta)$ where

$\phi_r(k\eta)$ is given by (IV.1). The contribution from DM is obtained from Einstein's equation (III.17) which for $a > a^*$ reduces to the Poisson's equation for all scales smaller than a few Mpc, namely

$$\phi_m(k,\eta) = -\frac{3}{4}\frac{k_{eq}^2}{k^2\,\tilde{a}}\,\delta(\vec{k},s)\,. \tag{IV.20}$$

For $s > s^*$ the integral in (IV.16) can be split up into the integral from s_{NR} up to s^* which is dominated by ϕ_r and corresponds to stage II, and the integral from s^* up to s in which the gravitational potential is dominated by the DM component (IV.20).

Therefore for $s > s^*$, the density perturbation δ obeys Gilbert's equation[57, 61, 83, 84]

$$\delta(\vec{k},s) = -\frac{9}{4}\frac{k_{eq}^2}{k^2\,\tilde{a}}\,\delta(\vec{k},s) + \frac{3}{2}\,H_0^2\,\Omega_m \int_{s^*}^{s} ds'(s-s')K(k,s-s')\,a(s')\,\delta(\vec{k},s') + I[k,s]\,, \tag{IV.21}$$

where the inhomogeneity

$$\begin{aligned} I[k,s] \;=\; & 3\phi_r(k,s) - k^2\int_{s_{NR}}^{s^*} ds' a^2(s')\phi_r(k,s')\,(s-s')\,K(k,s-s') \\ & + \int \frac{d^3p}{(2\pi)^3}\,p\left(\frac{d\widetilde{f}(p)}{dp}\right) e^{-i\frac{\vec{k}\cdot\vec{p}}{m}(s-s_{NR})}\;\mathcal{S}\big[\vec{k},\vec{p};\eta_{NR}\big]\,, \end{aligned} \tag{IV.22}$$

and ϕ_r is the radiation contribution to the gravitational potential given by (IV.1). Thus the inhomogeneity incorporates the *past history* during stages I and II.

C. Kernels for CDM and WDM:

The kernel $K(k, s-s')$ determines the suppression of WDM perturbations by non-relativistic free streaming and depends on the distribution function $\widetilde{f}(p)$. For WIMPs (CDM) $\widetilde{f}$ is the Maxwell-Boltzmann distribution function given by eqn. (III.9) whereas for (DW) or (BD) WDM particles $\widetilde{f}(y)$ is given by eqn. (III.7) or (III.8) respectively.

1. CDM: Maxwell-Boltzmann distribution function

For CDM we find

$$K(k,s-s') = e^{-\frac{\kappa^2}{6}(u-u')^2}\,, \tag{IV.23}$$

where $u(\eta)$ is defined by eqn. (III.32), and from the definitions (III.44,III.22), along with eqn. (III.23), we find

$$\kappa = \frac{\sqrt{6}\,k}{k_{fs}} = 0.38\,k\,\left(\frac{100\text{ GeV}}{m}\right)^{\frac{1}{2}}\left(\frac{10\text{ MeV}}{T_d}\right)^{\frac{1}{2}}\left(\frac{2}{g_d}\right)^{\frac{1}{3}}\times(pc)\,. \tag{IV.24}$$

2. WDM: DW distribution function

With the distribution function (III.7) one finds[57, 61, 84]

$$K(k, s-s') = K[Q] = \frac{4}{3\zeta(3)} \sum_{n=1}^{\infty} \frac{(-1)^{n+1}\, n}{(n^2+Q^2)^2} \tag{IV.25}$$

where

$$Q = \alpha\,(u-u') \;\;;\;\; \alpha = \frac{0.68\; k}{k_{fs}} = 0.278\,\kappa \tag{IV.26}$$

3. WDM: BD distribution function

With the distribution function (III.8) one finds[57]

$$K(k, s-s') = K[Q] = \frac{\sqrt{2}}{\sqrt{3}\,\zeta(5)} \sum_{n=1}^{\infty} \frac{1}{\Big(\rho\; n\Big)^{\frac{5}{2}}} \left[1+\frac{n}{\rho}\right]^{\frac{1}{2}} \left[\frac{2n+\rho}{n+\rho}\right] \;\;;\;\; \rho = \sqrt{n^2+Q^2}\,, \tag{IV.27}$$

where in this case

$$Q = \alpha(u-u')\;;\; \alpha = \frac{0.84\,k}{k_{fs}} = 0.343\,\kappa \tag{IV.28}$$

We note that in all the cases considered here, the kernels K are functions of the combination $\kappa^2(u-u')^2$.

The free streaming kernels are suppressed, either exponentially (MB) or as high inverse powers (DW,BD) of the ratio k^2/k_{fs}^2.

V. COLD DARK MATTER

For a WIMP of $m \sim 100$ GeV decoupling at $T_d \sim 10$ MeV (for which $g_d \sim 10$) comoving scales $\lambda \gg \eta_d \sim 10\,\mathrm{pc}$ entered the horizon well after decoupling and when the particle is non-relativistic, in which case we can set $\eta_{NR} \sim 0$ and

$$\Theta(k, \mu;\, \eta_{NR}) = \frac{1}{2}\,\phi_i(k)\,. \tag{V.1}$$

For these CDM particles, $\lambda_{fs} \lesssim 1\,\mathrm{pc}$ and for comoving wavelengths $\lambda \gg 10\,\mathrm{pc}$ it follows that $\kappa \ll 1$ therefore $K \simeq 1$, this amounts to setting $\langle V_{eq}^2\rangle^{\frac{1}{2}} = 0$, consistently with CDM. The perturbation equation (IV.16) simplifies to

$$\delta(\vec{k}, s) = 3\phi(k, s) - k^2 \int_{s_{NR}}^{s} ds' a^2(s')\phi(k, s')\,(s-s') - \frac{9}{2}\,\phi_i(k) \tag{V.2}$$

This equation can be recognized by taking d^2/ds^2 of both sides,

$$\frac{d^2}{ds^2}\left[\delta(\vec{k},s) - 3\phi(k,s)\right] = -k^2a^2\phi(k,s) \tag{V.3}$$

using $d/ds = ad/d\eta$ and $\dot{a}/a = 1/\eta$ during (RD) we find

$$\ddot{\delta} + \frac{\dot{\delta}}{\eta} = 3\ddot{\phi} + \frac{3}{\eta}\dot{\phi} - k^2\phi\,, \tag{V.4}$$

which is the equation obeyed by CDM perturbations during the (RD) era[76].

During this era when ϕ is determined by the radiation fluid $a^2(\eta) = [H_0^2\Omega_m a_{eq}]\eta^2$; $s(\eta) = \ln(\eta)/[H_0^2\Omega_m a_{eq}]^{\frac{1}{2}} + \text{constant}$ and $\phi(k,\eta)$ is given by eqn. (IV.1), and eqn. (V.2) becomes

$$\delta(k,\eta) = 9\,\phi_i(k)\left\{ -\left[\frac{x\cos(x) - \sin(x)}{x^3}\right] + \int_{x_{NR}}^{x} dx' \ln\left(\frac{x}{x'}\right)\,\frac{d}{dx'}\left(\frac{\sin(x')}{x'}\right) - \frac{1}{2}\right\} \tag{V.5}$$

where $x = k\eta/\sqrt{3}$. For WIMPs and perturbations with comoving scales $\lambda \gg 10\,\text{pc}$ we can set $x_{NR} = 0$, leading to the result

$$\delta(k,\eta) = -9\,\phi_i(k)\left\{ \left[\frac{x\cos(x) - \sin(x)}{x^3}\right] + \frac{\sin(x)}{x} - \frac{1}{2} - Ci(x) + \ln(x) + \gamma_E\right\} \tag{V.6}$$

where $\gamma_E = 0.577216\cdots$ and $Ci(x)$ is the cosine-integral function. Fig. (2) displays $\delta(x)/\delta(0)$ vs. $x = k\eta/\sqrt{3}$, where $\delta(0) = -3\phi_i(k)/2$. The density perturbation receives a "kick" upon entering the horizon at $k\eta \sim 1$. We find numerically that

$$\frac{\delta(x)}{\delta(0)} \simeq 6\left(\ln(x) + \gamma_E - \frac{1}{2}\right) \quad \text{for} \quad x \gtrsim 10\,. \tag{V.7}$$

We can now estimate the crossover scale at which the Newtonian potential is determined by radiation or CDM perturbations. For $\tilde{a} \ll 1$ deep in the RD dominated era and for subhorizon modes $k\eta \gg 1$ Einstein's equation (III.13) determines that

$$\left(\frac{\delta\rho}{\rho}\right)_r \sim 6\phi_i(k)\,\cos(x) \tag{V.8}$$

Taking the asymptotic behavior (V.7) for δ, the Newtonian potential determined by Einstein's equation (III.13) begins to be dominated by matter density perturbations when

$$\frac{3}{2}\,\tilde{a}\,\ln(x) > 1\,. \tag{V.9}$$

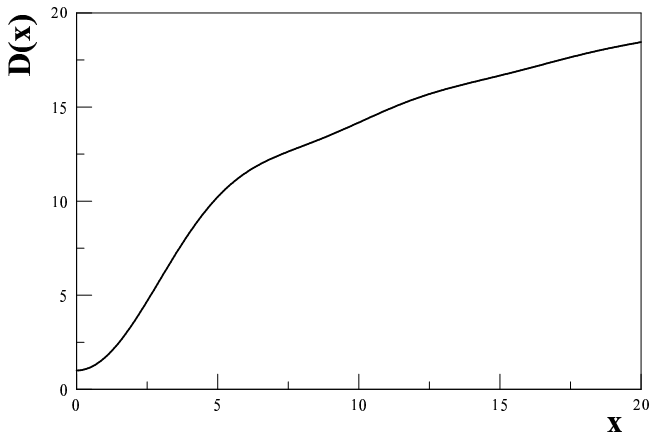

FIG. 2: $D(x) = \frac{\delta(x)}{\delta(0)}$ vs. $x = k\eta/\sqrt{3}$.

For comoving scales smaller than a few Mpc we find that the crossover scale from radiation to matter *perturbations* dominating the gravitational potential is

$$\tilde{a}^* \lesssim 0.1\,. \tag{V.10}$$

During RD, $x \sim \tilde{a}\sqrt{2}\,k/\sqrt{3}\,k_{eq}$, therefore for all comoving scales smaller than a few Mpc the crossover to the domination of the Newtonian potential by DM density perturbations occurs within the RD dominated era.

Passing to the variable u defined by eqn. (IV.12), for $u > u^*$ Gilbert's eqn. (IV.21) now becomes

$$\delta(\vec{k},u) = -\frac{9}{4}\frac{k_{eq}^2}{k^2\,\tilde{a}}\,\delta(\vec{k},u) + 6\int_{u^*}^{u} du'(u-u')\,\tilde{a}(u')\,\delta(\vec{k},u') + I[k,u] \tag{V.11}$$

where

$$I[k,u] = 3\phi_r(k,u) - \frac{8\,k^2}{k_{eq}^2}\int_{u_{NR}}^{u^*} du'\tilde{a}^2(u')\phi_r(k,u')\,(u-u') - \frac{9}{2}\,\phi_i(k)\,. \tag{V.12}$$

For $k \gg k_{eq}$ and $k\tilde{a} \gg k_{eq}$ which is valid for modes well inside the horizon when DM density perturbations dominate, we can safely neglect the first term (V.11) and because during radiation domination $k\eta = \sqrt{2}k\tilde{a}/k_{eq}$ and for modes deep inside the horizon $\phi_r \sim \cos(k\eta)/k^2\eta^2$ we can also neglect the $3\phi_r$ in $I[k,u]$. We then notice that $I[k,u]$ is linear in u and (V.11) can be turned into an ordinary homogenous differential equation,

$$\frac{d^2}{du^2}\,\delta(k,u) - 6\,\tilde{a}(u)\delta(k,u) = 0\,, \tag{V.13}$$

with the initial conditions

$$\delta(k,u^*) = I[k,u^*] \;\; ; \;\; \left.\frac{d\,\delta(k,u)}{du}\right|_{u=u^*} = \left.\frac{d\,I[k,u]}{du}\right|_{u=u^*} . \tag{V.14}$$

Since the variable u depends solely on the combination

$$\zeta = \sqrt{1+\tilde{a}(u)} = \frac{1}{\tanh[-u]} \tag{V.15}$$

(see eqn. (III.32)) it proves convenient to write the differential equation (V.13) in terms of ζ. We find

$$\frac{d}{d\zeta}\left[(1-\zeta^2)\,\frac{d\delta}{d\zeta}\right] + 6\,\delta = 0\,. \tag{V.16}$$

This is Legendre's equation of index $\nu = 2$ with solutions

$$P_2(\zeta) \;=\; \frac{1}{2}\,\left(3\,\zeta^2 - 1\right) \tag{V.17}$$

$$Q_2(\zeta) \;=\; \frac{1}{4}\left(3\,\zeta^2-1\right)\ln\left[\frac{\zeta+1}{\zeta-1}\right] - \frac{3}{2}\zeta \tag{V.18}$$

In terms of $\tilde{a}$ rather than ζ eqn. (V.16) becomes

$$\frac{d^2\,\delta}{d\tilde{a}^2} + \frac{(2+3\tilde{a})}{2\tilde{a}(1+\tilde{a})}\,\frac{d\delta}{d\tilde{a}} - \frac{3}{2}\frac{\delta}{\tilde{a}(1+\tilde{a})} = 0 \tag{V.19}$$

this is Meszaros' equation[69–71]. We find remarkable that in terms of the variable ζ Meszaros' equation is simply Legendre's equation of index $\nu = 2$.

The general solution is

$$\delta(k,\tilde{a}) = \delta_g(k) P_2(\zeta) + \delta_d(k) Q_2(\zeta) \;\; ; \;\; \zeta = \sqrt{1+\tilde{a}} \tag{V.20}$$

The coefficients $\delta_{g,d}$ must be obtained from the initial conditions (V.14) and the Wronskian of the independent solutions P_2, Q_2. However, we recognize that the asymptotic solution (V.7) can be written as

$$\delta(k,\tilde{a}) \simeq 6\,\delta_i\left[\ln\left(\frac{\sqrt{2}\,k\;e^{\gamma_E-\frac{1}{2}}}{\sqrt{3}\,k_{eq}}\right) + \ln\left[\zeta^2-1\right]\right] \tag{V.21}$$

where we used the relation $\eta = \sqrt{2}\tilde{a}/k_{eq}$ valid during the RD dominated era for $\eta \ll \eta_{eq}$ corresponding to $\tilde{a} \ll 1$. Matching (V.20) to (V.21) for $\zeta \sim 1$ we find

$$\delta_d(k) = -12\delta_i(k) \;\; ; \;\; \delta_g(k) = 6\delta_i(k)\ln\left[\frac{4\sqrt{2}\,k\;e^{\gamma_E-\frac{7}{2}}}{\sqrt{3}\,k_{eq}}\right] \tag{V.22}$$

For $\tilde{a} \gg 1$ the growing solution is given by $\delta_g P_2(\zeta)$, namely

$$\delta(k,\tilde{a}) \simeq 9\delta_i(k) \ln\left[\frac{4\sqrt{2}\,k\ e^{\gamma_E-\frac{7}{2}}}{\sqrt{3}\,k_{eq}}\right]\tilde{a} \tag{V.23}$$

and the gravitational potential becomes for $\tilde{a} \gg 1$

$$\phi(k) = \frac{9}{10}\,\phi_i(k)\,T_{CDM}(k)\,, \tag{V.24}$$

where including the long-wavelength normalization (III.69) we find

$$T_{CDM}(k) = \frac{45}{4}\frac{k_{eq}^2}{k^2}\ \ln\left[\frac{4\sqrt{2}\,k\ e^{\gamma_E-\frac{7}{2}}}{\sqrt{3}\,k_{eq}}\right] \tag{V.25}$$

is the CDM transfer function for $k \gg k_{eq}$. This result agrees with that of Weinberg[85] and Wu and Sugiyama[86] and numerically agrees to within few percent with the numerical fit provided by Bardeen *et.al.*[87] for $k \gg k_{eq}$.

An alternative derivation of this result which is relevant for comparison with WDM below begins by defining a new variable

$$\Delta(k,u) = \delta(k,u) - I[k,u] \tag{V.26}$$

obeying

$$\frac{d^2}{du^2}\,\Delta(k,u) - 6\,\tilde{a}(u)\Delta(k,u) = 6\,\tilde{a}(u)I[k,u]\,, \tag{V.27}$$

with initial conditions

$$\Delta(k,u^*) = 0\ \ ;\ \ \left.\frac{d\,\Delta(k,u)}{du}\right|_{u=u^*} = 0\,. \tag{V.28}$$

Therefore from the solution of (V.27,V.28) we find

$$\delta(k,u) = I[k,u] + 6\int_{u^*}^{u}\tilde{a}(u')I[k,u']\mathcal{G}(u,u')\,du' \tag{V.29}$$

where

$$\mathcal{G}(u,u') = \frac{1}{W}\Big[P(u)Q(u') - P(u')Q(u)\Big] \tag{V.30}$$

and $G[u,u'] = \mathcal{G}(u,u')\Theta(u-u')$ is the retarded Green's function obeying

$$\left[\frac{d^2}{du^2} - 6\,\tilde{a}(u)\right]G[u,u'] = \delta(u-u')\,. \tag{V.31}$$

The functions $P(u) = P_2(\zeta(u)); Q(u) = Q_2(\zeta(u))$ are the growing and decaying homogeneous solutions of

$$\left[\frac{d^2}{du^2} - 6\,\tilde{a}(u)\right]\left\{\begin{array}{c} P(u) \\ Q(u) \end{array}\right\} = 0\,, \tag{V.32}$$

and $W = 1$ their Wronskian. It is straightforward to prove that the solution (V.29) is exactly the same as (V.20) after using the homogeneous differential equation (V.32) for P_2, Q_2 and twice integrating by parts in u'.

Since the source $I[k,u]$ remains bound as $u \to 0^-$ ($\tilde{a} \to \infty$), it follows that asymptotically for $\tilde{a} \gg 1$

$$\delta(k,u) \to \frac{6}{W}\,P(u)\int_{u^*}^{0} Q(u')\,\tilde{a}(u')\,I[k,u']du' = 9\,\tilde{a}(u)\int_{u^*}^{0} Q_2(u')\,\tilde{a}(u')\,I[k,u']du'\,. \tag{V.33}$$

From (IV.20) and (III.69) we find

$$T_{CDM}(k) = -\frac{30}{4}\,\frac{k_{eq}^2}{k^2\,\phi_i(k)}\int_{u^*}^{0} Q_2(u')\tilde{a}(u')I[k,u']du'\,. \tag{V.34}$$

The main reason for describing this alternative in detail is because the form (V.34) generalizes to the WDM case.

VI. WARM DARK MATTER:

Passing to the dimensionless variable u in (IV.16), eqns. (IV.21,IV.22) become

$$\begin{aligned}\delta(\vec{k},u) \;=\; & 3\phi(k,u) - \frac{8k^2}{\alpha\,k_{eq}^2}\int_{u_{NR}}^{u} \tilde{a}^2(u')\,\phi(k,u')\,\Pi\big[\alpha(u-u')\big]\,du' \;+ \\ & \frac{1}{N}\int_0^\infty y^3 dy\Big(\frac{df_0(y)}{dy}\Big)\left\{\frac{3}{2}\phi_i(k)\,j_0\big[y\,\alpha(u-u_{NR})+z_{NR}\big]\right. \\ & \left. +\;2\int_0^{z_{NR}} dz'\phi(z')j_1\big[y\,\alpha(u-u_{NR})+z_{NR}-z'\big]\right\}\end{aligned} \tag{VI.1}$$

where

$$\Pi\big[\alpha(u-u')\big] = \frac{1}{N}\int_0^\infty y f_0(y)\sin\big[y\,\alpha\,(u-u')\big]\,dy \;= \alpha(u-u')K(k,u-u')\,, \tag{VI.2}$$

and N is defined in eqn. (IV.19).

When the DM perturbations dominate the gravitational potential for $u > u^*$ which is determined self-consistently as explained above, δ obeys Gilbert's equation in the form

$$\delta(\vec{k},u) - \frac{6}{\alpha}\int_{u^*}^{u}\tilde{a}(u')\,\delta(k,u')\,\Pi\big[\alpha(u-u')\big]\,du' \;=\; I[k;\alpha;u] \tag{VI.3}$$

where we neglected terms proportional to k_{eq}^2/k^2, and

$$I[k;\alpha;u] \;=\; 3\phi_r(k,u) - \frac{8k^2}{\alpha\, k_{eq}^2}\int_{u_{NR}}^{u^*} \tilde{a}^2(u')\,\phi_r(k,u')\,\Pi\big[\alpha(u-u')\big]\,du' \;+ \\ \frac{1}{N}\int_0^\infty y^3 dy\Big(\frac{df_0(y)}{dy}\Big)\left\{\frac{3}{2}\,\phi_i(k)\,j_0\big[y\,\alpha(u-u_{NR})+\frac{\kappa}{2}\big] \right. \\ \left. +\; 2\int_0^{\frac{\kappa}{2}} dz'\phi_r(z')j_1\big[y\,\alpha(u-u_{NR})+\frac{\kappa}{2}-z'\big]\right\}, \qquad \text{(VI.4)}$$

where we have used $z_{NR} = k\eta_{NR} = \kappa/2$. For $k \gg k_{eq}$ the term $3\phi_r$ in the first line in (VI.4) is subleading as compared to the second term and will also be neglected in our analysis.

It is clear from the integral equation (VI.3) that δ obeys the initial conditions

$$\delta(k,u^*) = I[k;\alpha;u^*] \;\;;\;\; \frac{d\,\delta(k,u)}{du}\bigg|_{u^*} = \frac{d\,I[k;\alpha;u]}{du}\bigg|_{u^*}. \qquad \text{(VI.5)}$$

In the first line in (VI.4) the kernel Π determines the free streaming of WDM perturbations during the (RD) stage during which the particle is *non-relativistic*, whereas the last two lines are the result of free streaming during the stage when the particle is still *relativistic*. In particular the third term in (VI.4) corresponds to the ISW contribution (IV.5) (after an integration by parts) studied in section (IV A) which undergoes damping by free streaming during the non-relativistic stage. As it will be seen below, this ISW contribution yields an *enhancement* of the transfer function for $k < k_{fs}$.

Thus the inhomogeneity $I[k;\kappa;u]$ is completely determined by the past history during stages I and II when perturbations in the radiation component dominate the gravitational potential. We have made explicit that the inhomogeneity depends both on k and α (or κ). For fixed wavevector k the CDM limit is obtained by letting $m(g_d)^{\frac{1}{3}} \to \infty$ which lets $\alpha \to 0$ (and $\kappa \to 0$) with fixed k (see the definition (III.22)) and also $u_{NR} \to -\infty$ ($\eta_{NR} \to 0$).

At this stage one can proceed to a numerical integration of (VI.3), however in this article we will pursue an approximate semi-analytic treatment valid for an *arbitrary distribution function* postponing a full numerical study to a forthcoming article.

Before studying (VI.3,VI.4), we analyze the asymptotic long time behavior as $u \to 0$ of the WDM density perturbation, which is obtained by neglecting the source term I since it is bounded in time.

For $u \to 0$ it follows from (III.35) that $\tilde{a}(u) \simeq 1/u^2$. The integrand in (VI.3) is dominated by the region $u' \sim u \sim 0$, assuming that $\delta(k,u) \to \delta(k,0)(-u)^{-\beta}$ as $u \to 0$ and using that

for $u' \sim u \sim 0$ it follows that $\Pi[\alpha(u-u')] \sim \alpha(u-u')$, and we find

$$\frac{6}{\alpha}\int_{u^*}^{u} \tilde{a}(u')\,\delta(k,u')\,\Pi\big[\alpha(u-u')\big]\,du' \sim \delta(k,0)\frac{6\,(-u)^{\beta}}{\beta(\beta+1)} \tag{VI.6}$$

therefore there is a self-consistent solution of eqn. (VI.3) (for $I=0$) with $\beta = 2, -3$ corresponding to the growing and decaying solutions $\delta_g(k,u) \propto \tilde{a}\,;\, \delta_d(k,u) \propto 1/\tilde{a}^{3/2}$ respectively. This is an *exact* result which shows that asymptotically for $\tilde{a} \gg 1$ $\delta \propto \tilde{a}$.

The Volterra equation of the second kind (VI.3) has a solution in terms of the Fredholm-Neumann series. However this iterative solution does not make explicit the growth factor $\tilde{a}$ exhibited by the exact solution. The analysis of the CDM case in the previous section suggests a re-organization of this series that manifestly exhibits the growth factor. For this purpose we cast Gilbert's equation (VI.3) as an integro-differential equation by taking derivatives with respect to u.

The following integro-differential equation is obtained,

$$\frac{d^2}{du^2}\delta(k,u) - 6\tilde{a}(u)\delta(k,u) - \frac{6}{\alpha}\int_{u^*}^{u} \tilde{a}(u')\,\delta(k,u')\,\frac{d^2}{du^2}\Pi\big[\alpha(u-u')\big]\,du' = \frac{d^2}{du^2}I[k,u]\,. \tag{VI.7}$$

Performing the same asymptotic analysis in the limit $u \to 0; \tilde{a}(u) \sim 1/u^2$ leading to (VI.6) we find in this limit[3]

$$-\frac{6}{\alpha}\int_{u^*}^{u} \tilde{a}(u')\,\delta(k,u')\,\frac{d^2}{du^2}\Pi\big[\alpha(u-u')\big]\,du' \sim \alpha^2\,\overline{y^2}\,\delta(k,u) \;\;;\;\; \overline{y^2} = \frac{1}{N}\int_0^{\infty} y^4 f_0(y)dy\,. \tag{VI.8}$$

This leading asymptotic behavior can be incorporated in (VI.7) by writing

$$\frac{d^2}{du^2}\Pi\big[\alpha(u-u')\big] = -\alpha^2\overline{y^2}\,\Pi\big[\alpha(u-u')\big] + \alpha^2\widetilde{\Pi}\big[\alpha(u-u')\big] \tag{VI.9}$$

where

$$\widetilde{\Pi}\big[\alpha(u-u')\big] = \frac{1}{N}\int_0^{\infty} y f_0(y)(\overline{y^2}-y^2)\sin\big[y\,\alpha\,(u-u')\big]dy \tag{VI.10}$$

Using the original integral equation (VI.3) we obtain

$$\begin{aligned}&\frac{d^2}{du^2}\delta(k,u) - 6\tilde{a}(u)\delta(k,u) + \kappa^2\delta(k,u) - 6\,\alpha\int_{u^*}^{u} \tilde{a}(u')\,\widetilde{\Pi}\big[\alpha(u-u')\big]\delta(k,u')\,du' \\ =\;& \frac{d^2}{du^2}I[k,u] + \kappa^2 I[k,u]\end{aligned} \tag{VI.11}$$

[3] This can be found self-consistently by proposing $\delta(k,u) \propto (-u)^{-\beta}$ and following the steps leading to (VI.6.)

were we used the definition (III.44).

The last term in the first line in (VI.11) can be interpreted as a non-local potential with a memory kernel $\widetilde{\Pi}\big[\alpha(u-u')\big]$. It is straightforward to show that $\widetilde{\Pi}\big[\alpha(u-u')\big] \propto (u-u')^3$ as $u' \to u$ and from the results for the kernels (IV.23,IV.25,IV.27) that it falls off as a high power (or exponential) of the argument for the distribution functions considered here.

Furthermore, we have already established that asymptotically $\delta(k,u) \propto \tilde{a} \propto 1/u^2$, implementing the same analysis leading to (VI.6) and replacing this asymptotic behavior in the memory integral in (VI.11) we find that asymptotically as $u \to 0$ it behaves as

$$\int_{u^*}^{u} \tilde{a}(u')\,\widetilde{\Pi}\big[\alpha(u-u')\big]\delta(k,u')\,du' \propto \ln(-u) \propto \ln(\tilde{a})\,, \tag{VI.12}$$

therefore its contribution is *subleading* in the asymptotic limit $\tilde{a} \to \infty$ as compared to all the other terms in the first line of (VI.11).

Hence, we conclude from this analysis that the memory integral in (VI.11) can be considered as a *perturbation*.

Again, it is convenient to introduce the combination $\Delta(k,u)$ given by (V.26) that satisfies

$$\frac{d^2}{du^2}\Delta(k,u) - 6\tilde{a}(u)\Delta(k,u) + \kappa^2\Delta(k,u) = 6\tilde{a}(u)I[k,u] + \mathcal{J}[\delta;u] \tag{VI.13}$$

with the initial conditions given by (V.28), where

$$\mathcal{J}[\delta;u] = 6\,\alpha\int_{u^*}^{u} \tilde{a}(u')\,\widetilde{\Pi}\big[\alpha(u-u')\big]\delta(k,u')\,du'\,. \tag{VI.14}$$

The solution of (VI.13) with the initial conditions (V.28) is completely determined by the retarded Green's function obeying

$$\left[\frac{d^2}{du^2} - 6\tilde{a}(u) + \kappa^2\right] G[u,u'] = \delta(u-u')\,. \tag{VI.15}$$

The formal solution of (VI.11) with initial conditions (VI.5) is

$$\delta(k,u) = I[k,u] + \int_{u^*}^{u} \mathcal{G}(u,u')\left[6\tilde{a}(u')I[k,u'] + \mathcal{J}[\delta;u']\right]du' \tag{VI.16}$$

where

$$\mathcal{G}(u,u') = \frac{1}{W}\Big[P(u)\,Q(u') - P(u')\,Q(u)\Big] \tag{VI.17}$$

where P, Q are the linearly independent growing and decaying homogeneous solutions of the fluid-like equation

$$\left[\frac{d^2}{du^2} - 6\,\tilde{a}(u) + \kappa^2\right]\left\{\begin{array}{c} P(\kappa;u) \\ Q(\kappa;u) \end{array}\right\} = 0 \tag{VI.18}$$

and W is their (constant) Wronskian. The formal solution (VI.16) is again an integral equation, however it is a re-summed form of the Fredholm-Neumann solution of (VI.3) that displays the asymptotic growth factor explicitly since asymptotically the growing solution of (VI.18) $P(\kappa;u)$ features the growth factor $\propto \tilde{a}$ (see below).

From the analysis above, we note that the inhomogeneity $\mathcal{J}$ is *subleading* compared to the first term $\tilde{a}\, I[k,u]$ for the following reasons:

- At early times $u \sim u^*$, $\mathcal{J}$ vanishes as $(u-u^*)^3$ whereas $\tilde{a}\, I[k,u]$ remains finite.
- Asymptotically at long time $(u \to 0; \tilde{a} \to \infty)$ $\tilde{a}\, I[k,u] \sim \tilde{a} I[k,0] \propto \tilde{a}$ whereas $\mathcal{J} \propto \ln(\tilde{a})$.
- At long wavelengths $k \to 0$ for which $\alpha \to 0$ $(\kappa \to 0)$ it follows that $\mathcal{J} \to 0$. This is the CDM limit.
- For short wavelengths free streaming suppresses density perturbations, this is manifest in the expression (VI.4). In an iterative solution δ is suppressed by free streaming and the term $\mathcal{J}$ involves a further suppression by the kernel $\widetilde{\Pi}$ with respect to I.

Hence the term $\mathcal{J}$ can be treated perturbatively as argued above, giving rise to a systematic Fredholm-Neumann iterative solution of (VI.16) formally in powers of the free streaming kernels Π which for (WDM) are strongly suppressed by large inverse powers of κ at small wavelength (see the expressions (IV.23-IV.27) or exponentially suppressed as for (MB) (see (IV.23))

$$\delta(k,u) = \delta^{(0)}(k,u) + \delta^{(1)}(k,u) + \cdots \tag{VI.19}$$

where

$$\delta^{(0)}(k,u) \;=\; I[k,u] + 6\int_{u^*}^{u} \mathcal{G}(u,u')\tilde{a}(u')I[k,u'] \tag{VI.20}$$

$$\delta^{(n)}(k,u) \;=\; \int_{u^*}^{u} \mathcal{G}(u,u')\mathcal{J}[\delta^{(n-1)};u']du' \;; n \geq 1 \tag{VI.21}$$

note that $\delta^{(0)}(k,u)$ is first order in the free streaming kernels, $\delta^{(1)}(k,u)$ second order, etc.

We refer to the zeroth-order solution (VI.20) as the *Born approximation* because of its similarity to quantum scattering theory. In references [57, 61] it was shown that the Born approximation is reliable in a wide range of scales. In what follows we will study the transfer

function in the Born approximation as a prelude to a full numerical study of (VI.3) and its comparison to the Born and higher approximations to be reported elsewhere.

We note that the Born approximation is *exact* for CDM since in this case $\alpha = 0$ (consequently $\kappa = 0$).

It remains to obtain the homogeneous solutions P, Q of the fluid-like equation (VI.18), which becomes more familiar when written in terms of cosmic time t,

$$\left[\frac{d^2}{dt^2} + 2H\frac{d}{dt} + \left(\frac{k^2\,\langle V^2(t)\rangle}{a^2(t)} - 4\pi\rho_m(t)\right)\right]\left\{\begin{array}{c} P \\ Q \end{array}\right\} = 0 \qquad \text{(VI.22)}$$

where $\rho_m(t); \langle V^2(t)\rangle$ are the density and the velocity squared velocity dispersion of the DM particle given by (III.37,III.38). This is equivalent to the Jean's fluid equation for non-relativistic matter recognizing that $k/a(t) = k_{phys}(t)$ is the physical wavevector, and replacing the (adiabatic) speed of sound by the DM particle's velocity dispersion. The term proportional to k^2 plays the role of a pressure term and its origin is traced back to the free-streaming kernel Π in Gilbert's equation (VI.3).

We emphasize that whereas the fluid equation (VI.22) suggests acoustic-like oscillations and is familiar, it is only *half the story*, it has *no information* on the suppression of perturbations by free streaming. The solution of Gilbert's equation (VI.19,VI.20,VI.21) is completely determined by the inhomogeneity and initial conditions, these are determined by the past history and describe the suppression of density perturbations by free-streaming.

A. Meszaros' equation for WDM

Just as in the CDM case (see equations (V.13,V.16)), it is convenient to pass to the variable ζ, in terms of which the homogeneous equation (VI.18) becomes

$$\left[(1-\zeta^2)\,\frac{d^2}{d\zeta^2} - 2\,\zeta\,\frac{d}{d\zeta} + \nu(\nu+1)\; - \frac{(i\kappa)^2}{1-\zeta^2}\right]\left\{\begin{array}{c} P(\kappa,\zeta) \\ Q(\kappa,\zeta) \end{array}\right\} = 0 \;\;;\;\; \nu = 2 \qquad \text{(VI.23)}$$

this is the associated Legendre equation with indices $\nu = 2\,;\, i\kappa$. We choose the growing and decaying solutions respectively as

$$P(\kappa,\zeta) = \mathrm{Re}\left\{\left(\frac{\zeta-1}{\zeta+1}\right)^{\frac{-i\kappa}{2}} F\Big[-2, 3; 1-i\kappa; \frac{1-\zeta}{2}\Big]\right\} \qquad \text{(VI.24)}$$

$$Q(\kappa,\zeta)=\frac{\sinh(\pi\kappa)}{2\pi\kappa}\mathrm{Re}\left\{\Gamma(3-i\kappa)\Gamma(i\kappa)\left(\frac{\zeta-1}{\zeta+1}\right)^{\frac{-i\kappa}{2}}F\Big[-2,3;1-i\kappa;\frac{1-\zeta}{2}\Big]\right\} \tag{VI.25}$$

where $F[a,b;c;z]$ is the hypergeometric function. We find

$$P(\kappa,u)=\cos(\kappa\,u)\,F_R(\kappa,\zeta(u))+\kappa\sin(\kappa\,u)\,H(\kappa,\zeta(u)) \tag{VI.26}$$

$$Q(\kappa,u)=-\frac{1}{2}\left\{3P(\kappa,u)+(\kappa^2-2)\left[\cos(\kappa\,u)\,H(\kappa,\zeta(u))-\frac{\sin(\kappa\,u)}{\kappa}\,F_R(\kappa,\zeta(u))\right]\right\} \tag{VI.27}$$

where

$$F_R(\kappa,\zeta(u))=1-\frac{3(1-\zeta)}{(1+\kappa^2)}+\frac{3(2-\kappa^2)(1-\zeta)^2}{(1+\kappa^2)(4+\kappa^2)} \tag{VI.28}$$

$$H(\kappa,\zeta)=-\frac{3(1-\zeta)}{(1+\kappa^2)(4+\kappa^2)}\left[1+\kappa^2+3\,\zeta\right]\;\;;\;\;\zeta(u)=\frac{1}{\tanh[-u]} \tag{VI.29}$$

It is straightforward to confirm that $P(0,\zeta)=P_2(\zeta)\;\;;\;\;Q(0,\zeta)=Q_2(\zeta)$ are the Legendre functions solutions of Meszaros's equation (V.17,V.18) for CDM perturbations. In fact, in terms of the variable $\tilde{a}$ equation (VI.18) (or alternatively eqn. (VI.23)) becomes *Meszaro's equation for WDM*,

$$\left[\frac{d^2}{d\tilde{a}^2}+\frac{(2+3\tilde{a})}{2\tilde{a}(1+\tilde{a})}\,\frac{d}{d\tilde{a}}-\frac{3}{2\tilde{a}(1+\tilde{a})}+\frac{\kappa^2}{4\tilde{a}^2(1+\tilde{a})}\right]\left\{\begin{array}{c}P\\ \\ Q\end{array}\right\}=0 \tag{VI.30}$$

whose growing and decaying solutions are given by (VI.26,VI.27) respectively.

The asymptotic behavior of the growing and decaying solutions for $\tilde{a}\gg 1\;;\;u\to 0$ are

$$P(\kappa,u)\;\to\;\frac{3(2-\kappa^2)}{u^2\,(1+\kappa^2)(4+\kappa^2)} \tag{VI.31}$$

$$Q(\kappa,u)\;\to\;\frac{-u^3\,(1+\kappa^2)(4+\kappa^2)}{30} \tag{VI.32}$$

from which we extract the Wronskian

$$W=\frac{2-\kappa^2}{2}\,. \tag{VI.33}$$

Therefore we find

$$\mathcal{G}(u,u')=\frac{2}{2-\kappa^2}\left[P(\kappa,u)\,Q(\kappa,u')-P(\kappa,u')\,Q(\kappa,u)\right]. \tag{VI.34}$$

For $\tilde{a}\gg 1$ when the gravitational potential is determined by DM perturbations, using Poisson's equation (IV.20), the definition of the transfer function (III.69) and the solution

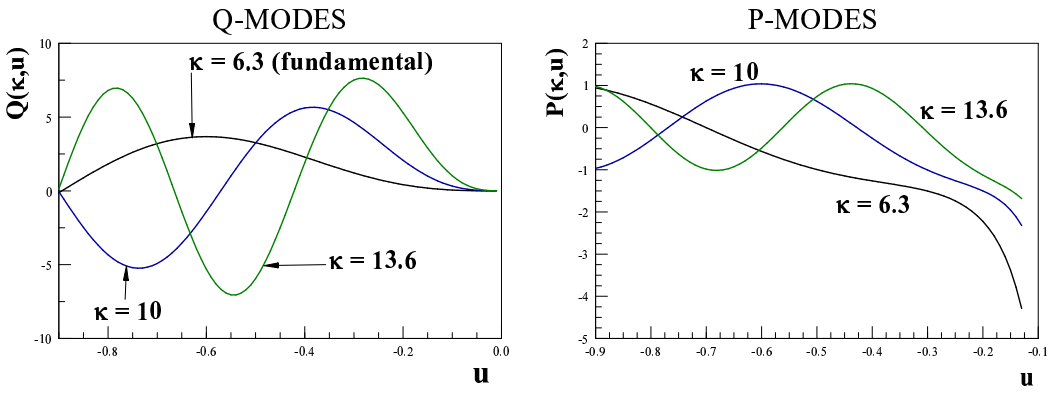

FIG. 3: Mode functions of fluid equation (VI.18). $Q(\kappa, u)$ are the decaying and $P(\kappa, u)$ the growing solutions. The "fundamental" decaying solution features a node at matter-radiation equality.

for δ (VI.16) along with the asymptotic behavior (VI.31) of the growing solution $P(\kappa, u)$ leads to an *exact* expression for the transfer function

$$T_{WDM}(k;\kappa) = \frac{-5\, k_{eq}^2}{k^2(1+\kappa^2)(4+\kappa^2)\,\phi_i(k)} \int_{u^*}^{0} Q(\kappa,u') \left[6\tilde{a}(u') I[k;\kappa;u'] + \mathcal{J}[\delta;u'] \right] du' \,. \tag{VI.35}$$

The CDM transfer function $T_{CDM}(k)$ corresponds to setting $\alpha = 0; \eta_{NR} \to 0$ which sets $\kappa = 0; u_{NR} \to -\infty$ and $\mathcal{J} = 0$. In the Born approximation we obtain

$$T_B(k;\kappa) = \frac{-30\, k_{eq}^2}{k^2(1+\kappa^2)(4+\kappa^2)\,\phi_i(k)} \int_{u^*}^{0} Q(\kappa,u')\, \tilde{a}(u') I[k;\kappa;u'] du' \tag{VI.36}$$

and as explained above the Born approximation is *exact* for CDM (for $k \gg k_{eq}$).

$T_{CDM}(k)$ is given by (V.34) and its leading behavior for $k \gg k_{eq}$ is given by (V.25). It is convenient to normalize the WDM transfer function defining

$$\overline{T}(k) = \frac{T_{WDM}(k;\kappa)}{T_{CDM}(k)} \tag{VI.37}$$

where WDM refers to $\kappa \neq 0$. In the Born approximation we find

$$\overline{T}_B(k) = \frac{4}{(1+\kappa^2)(4+\kappa^2)} \left[\frac{\int_{u^*}^{0} Q(\kappa,u')\, \tilde{a}(u') I[k;\kappa;u']\, du'}{\int_{u^*}^{0} Q_2(u')\, \tilde{a}(u') I^{CDM}[k;u']\, du'} \right] \tag{VI.38}$$

where Q_2 is the Legendre function given by eqn. (V.18),

$$\tilde{a}(u) = \frac{1}{\sinh^2[u]} \,, \tag{VI.39}$$

and

$$I^{CDM}[k;u] = I[k;0;u]\,. \tag{VI.40}$$

The matching scale u^* describes the transition from when the gravitational potential is dominated by the radiation fluid to when the DM perturbations dominate. In the CDM case analyzed in section(V) we found that this scale is smaller than the scale of matter-radiation equality. From the result (V.7) and the analysis leading to (V.21) we also found that the density perturbation in CDM depends logarithmically on the change of scale and for $k \gg k_{eq}$ taking the matching scale

$$u^* \simeq u_{eq} = \frac{1}{2}\,\ln\left[\frac{\sqrt{2}-1}{\sqrt{2}+1}\right] = -0.881 \tag{VI.41}$$

yields a correction which is of order $k_{eq}^2/k^2 \ll 1$ in the small scale regime studied here. For WDM, free streaming makes the dependence on this scale even weaker, and it is evident from the expression (VI.38) that the contribution from $\tilde{a} \ll 1$ is suppressed. Hence, in our analysis we take $u^* = u_{eq} = -0.881$. A comprehensive numerical analysis confirms the insensitivity on the choice of scale for $k \gg k_{eq}$.

It is convenient to divide the inhomogeneity (VI.4) by $-3\phi_i(k)$ which cancels in the ratio (VI.36). Furthermore since the integrals in (VI.36) range from $\eta_{eq} \leqslant \eta \leqslant \infty$ and $\phi(k,\eta) \propto 1/(k\eta)^2$ we can safely neglect the term $3\phi_r$ in the first line in (VI.4) as compared to the second term for $k \gg k_{eq}$. Thus in the ratio (VI.36) I simplifies to

$$\widetilde{I}[k;\alpha;u] = \frac{1}{N}\int y^2 f_0(y)\Big[I_1[k;y;u] + I_2[k;y;u] + I_{ISW}[k;y;u]\Big]dy \tag{VI.42}$$

where

$$I_1[k;y;u] = -\frac{8\,k^2}{k_{eq}^2}\int_{u_{NR}}^{u_{eq}} \tilde{a}^2(u')\,\varphi(k;u')\frac{\sin[y\alpha(u-u')]}{y\alpha}du'\,, \tag{VI.43}$$

$$I_2[k;y;u] = \frac{d\ln f_0(y)}{d\ln y}\Big[-\frac{1}{2}\,j_0\Big(y\alpha(u-u_{NR})+\frac{\kappa}{2}\Big)\Big] \tag{VI.44}$$

$$I_{ISW}[k;y;u] = \frac{d\ln f_0(y)}{d\ln y}\left[2\int_0^{\frac{\kappa}{2}}\varphi(z')j_1\Big(y\alpha(u-u_{NR})+\frac{\kappa}{2}-z'\Big)\right]dz' \tag{VI.45}$$

where

$$\varphi(z) = \left[\frac{\big(\frac{z}{\sqrt{3}}\big)\,\cos\big(\frac{z}{\sqrt{3}}\big) - \sin\big(\frac{z}{\sqrt{3}}\big)}{\big(\frac{z}{\sqrt{3}}\big)^3}\right] \quad ; \quad z = k\,\eta\,. \tag{VI.46}$$

In the CDM limit ($\alpha \to 0$)

$$\frac{\sin[y\alpha(u-u')]}{y\alpha} \to (u-u') \quad ; \quad I_2 \to -\frac{1}{2}\frac{d\ln f_0(y)}{d\ln y} \quad ; \quad I_{ISW} \to 0\,, \tag{VI.47}$$

leading to

$$\widetilde{I}^{CDM}[k;u] = -\frac{8\,k^2}{k_{eq}^2}\int_{u_{NR}}^{u_{eq}} \tilde{a}^2(u')\,\varphi(k;u')\,(u-u')\,du' + \frac{3}{2}\,, \tag{VI.48}$$

which along with (V.18) determines the denominator in (VI.36).

In the appendix we provide an explicit form for (VI.43), we gather all the relevant results, and provide a concise summary of the Born approximation for an easy numerical implementation.

The contribution I_{ISW} is a result of an integration by parts in eqn.(IV.3) and is the only contribution that vanishes in the CDM limit. It originates in stage I during (RD) when the WDM particle is still relativistic.

Figures (4,5) displays the ratio $\overline{T}$ and its logarithm for both cases of non-resonant sterile neutrino production (DW,BD). The production via boson decay at the electroweak scale leads to a *colder* species for two reasons: i) the effective number of degrees of freedom at decoupling g_d is larger, therefore the particle is colder today and at matter-radiation equality, and ii) the distribution function (III.8) favors small momenta and yields a smaller velocity dispersion (see eqn. (III.23)). This is manifest in the transfer functions displayed in fig. (4): it is clear from this figure that the wavevector scale of suppression for DW-produced sterile neutrinos is smaller than for the BD-production mechanism for the same mass.

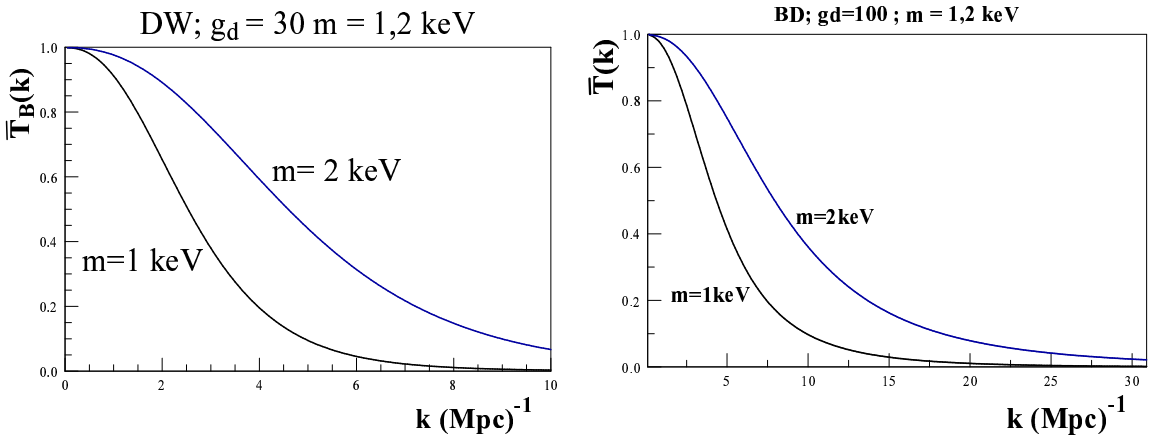

FIG. 4: $\overline{T}_B(k)$ for DW, and BD for m=1,2 keV. Sterile neutrinos produced via the BD-non-resonant mechanism are colder for the same mass.

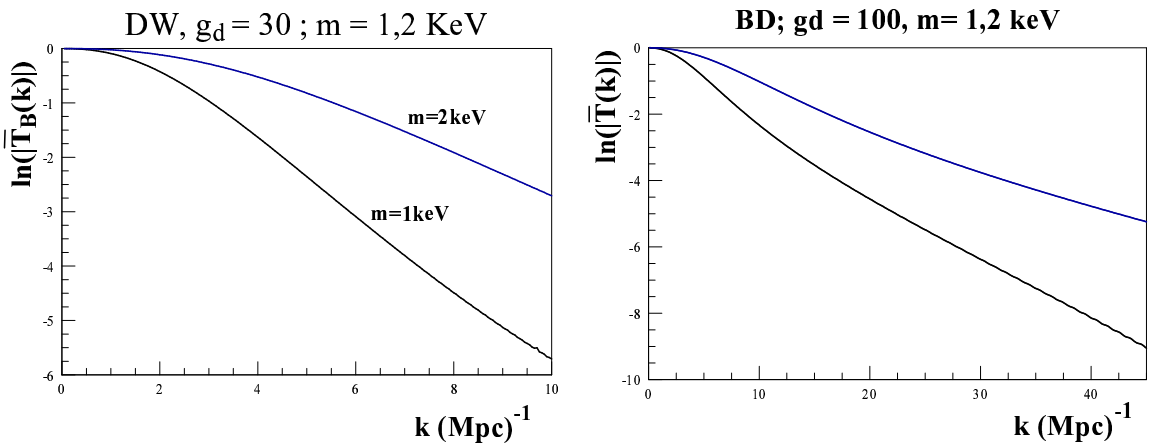

FIG. 5: $\ln(|\overline{T}_B(k)|)$ a for DW and BD, for m=1,2 keV.

B. ISW enhancement:

As discussed above the contribution I_{ISW} is a direct consequence of the evolution of density perturbations during stage I during the (RD) era described by eqn. (IV.3), and vanishes in the CDM limit. Therefore it is a distinct contribution to the WDM transfer function, and only arises from the time evolution of the Newtonian potential driven by the acoustic oscillations of the radiation fluid, i.e. an ISW effect.

This contribution is "out of phase" with the first two terms $I_{1,2}$: the Bessel functions j_0 of these two terms are decreasing functions of k until their arguments vanish. Instead, the Bessel function j_1 grows during the initial interval when j_0 decreases. As a result I_{ISW} grows for small k. This is precisely the behavior displayed in fig. (1) corresponding to the $l = 0$ (monopole) component of the density perturbation (IV.5) (integrating by parts the integral term the j_0 becomes j_1).

Since the maximum value of η during stage I is η_{NR} and $k\eta_{NR} = \kappa/2$ the analysis following eqn. (IV.8) suggests that I_{ISW} features a peak when the wavelength of the perturbation is approximately the sound horizon at η_{NR}, namely $k\eta_{NR} \approx \sqrt{3}\pi$ or $\kappa \approx 2\pi\sqrt{3}$. This analysis suggests that I_{ISW} features a peak at $k \lesssim k_{fs}$ because the argument of the Bessel function is now shifted towards the positive values (since $u - u_{NR} \geq 0$). The presence of a peak can also be gleaned from I_{ISW} directly, since for small z' $\varphi(z')$ is nearly constant but j_1 grows, featuring a maximum when its argument is ≈ 2, which obviously suggests a peak at $k \approx k_{fs}$. Therefore the hotter species, with smaller k_{fs} must feature a peak at a *smaller* value of k

when compared to the colder species which features the peak at a larger value k because of a larger value of k_{fs}. This expectation is borne out by fig. (6) that displays the ISW contribution to the Born ratio $\overline{T}_B$ (VI.38). The ISW enhancement extends to larger values of k for the colder species for the same mass (BD) as a consequence of a larger value of k_{fs}.

For small k the contributions I_2 and I_{ISW} feature opposite signs, therefore the ISW enhancement competes with and is partially cancelled by I_2 yielding an overall suppression of the transfer function with respect to CDM. Nevertheless, the ISW enhancement prolongs the region in k where the transfer function is closer to that of CDM.

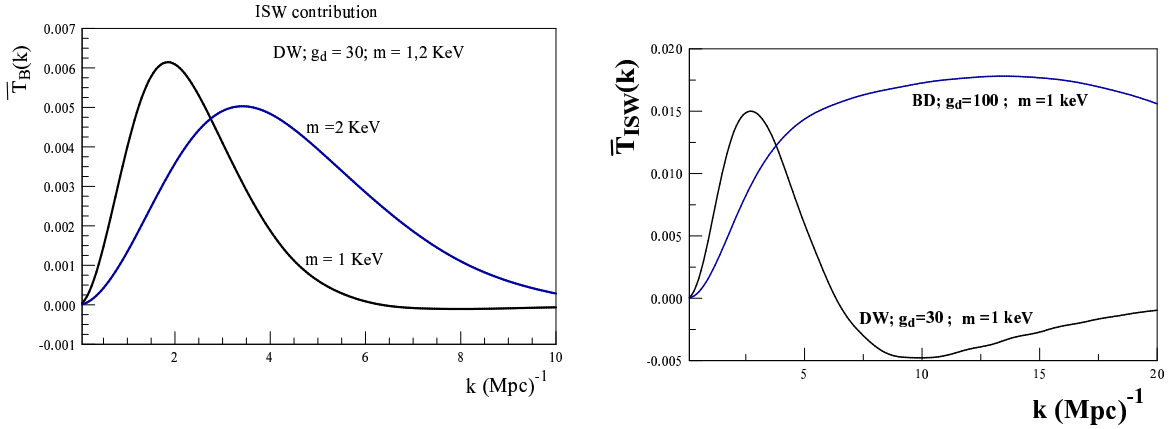

FIG. 6: The ISW contribution to $\overline{T}_B(k)$ for DW, m=1,2 keV and comparison with BD for m=1 keV.

For $\kappa \gtrsim 30$ ($k \gg k_{fs}$) the ISW contribution features oscillations as discussed in section (IV A) and shown explicitly in fig. (1).

C. On the origin of WDM acoustic oscillations:

The Q and P modes (VI.27,VI.26) feature acoustic oscillations as displayed in fig. (3), and only the Q modes enter in the evaluation of the transfer function (VI.36). This mode function always vanishes at $u = 0$ (today), and there is a particular "fundamental" mode that features only one other node at matter-radiation equality, for $\kappa \simeq 6.3$. In the integral leading to the transfer function (VI.36) the mode function Q multiplies the three contributions to I displayed in (VI.42-VI.45). The integral over y with the distribution function leads to the dephasing of the oscillatory functions in I_1, I_2, I_{ISW} and their suppression by free streaming.

However, we can identify some of the more obvious oscillatory contributions. From the study in section (IV A) and the results displayed in fig. (1), the oscillations from the ISW component begin at $z_{NR} \gtrsim 15$ ($\kappa \gtrsim 30$) or $k \gtrsim 5\sqrt{6}\, k_{fs}$, and are suppressed by free streaming during stages II) and III). This suppression is encoded in the y integral with the distribution function which contributes during the stages when the particle is non-relativistic.

The explicit form of I_1 given in the appendix, (A.7) reveals at least two contributions that lead to oscillations, these are the term $\sin[\alpha\, y\, U]/\alpha\, y$ in the first line, and the second line in (A.7). After integrating in y these contributions are proportional to the free streaming kernels (IV.23,IV.25,IV.27), however, although these contributions do *not* feature oscillations after the integration in y by themselves, they are multiplied by the mode function Q. Therefore the last term in the first line in (A.7) leads to oscillations for wavevectors larger than that of the "fundamental" Q-mode. The second line in (A.7) yields a contribution of the form

$$\propto \Big[1 - \frac{\sin(x_{NR})}{x_{NR}}\Big]$$

times a function suppressed by free streaming. With $x_{NR} = \kappa/2$ this contribution vanishes for $k \ll k_{fs}$, reaches the value 1 at $\kappa = 2\pi$ and oscillates around one for $\kappa \gg 2\pi$. Therefore this function reaches its asymptotic value ~ 1 for values of κ near the "fundamental" mode. This analysis leads us to suggest that oscillations in the transfer function begin when the "fundamental" mode is excited, namely $\kappa \gtrsim 6.3$.

For values of $\kappa \gtrsim 6.3$ the nodes in the mode functions Q between matter-radiation equality and today lead to oscillations in the transfer functions. Therefore we conclude that oscillations are manifest for

$$k \gtrsim 2\ k_{fs}\,. \tag{VI.49}$$

This expectation is approximately borne out, for (DW) with $k_{fs} \sim 7.7\,(\mathrm{Mpc})^{-1}$ we see from fig. (7) that oscillations begin at $k \approx 11\,(\mathrm{Mpc})^{-1}$ and for (BD) with $k_{fs} \approx 14\,(\mathrm{Mpc})^{-1}$, fig. (8) shows oscillations beginning at $k \approx 31.5\,(\mathrm{Mpc})^{-1}$. The period of the oscillations is more difficult to assess because the various terms are out of phase leading to beating of frequencies (a hint of this is observed in $\ln(\overline{T})$ displayed in fig. (7)), however, the approximate estimate $k \simeq 2\, k_{fs}$ for the emergence of oscillations is confirmed by the numerical analysis.

It is important to recognize that both I_1, I_{ISW} originate in the acoustic oscillations of the radiation fluid, which couple to the WDM perturbations via the Newtonian potential.

Therefore in this sense, the origin of the WDM acoustic oscillations at small scales is similar to the small scale oscillations in the CDM transfer function obtained in ref.[74]. In that reference the oscillations originated from the *direct coupling* of the CDM particle to the radiation fluid prior to decoupling, whereas in this work the coupling is *indirect* through the gravitational potential and the *past history* of the evolution during stages I and II.

At the scale where WDM acoustic oscillations emerge the transfer function is strongly suppressed by free-streaming and as a result of this suppression in the power spectrum the relevance of these WDM acoustic oscillations for structure formation is not clear. However, it is conceivable that the effect of the oscillations will be amplified by non-linear gravitational collapse, leading to enhanced peaks and troughs in the matter distribution at low redshift.

The (comoving) scales for these oscillations $k_{ao} \sim 11\,(\mathrm{Mpc})^{-1}$ for (DW) and $k_{ao} \sim 31.5\,(\mathrm{Mpc})^{-1}$ for (BD) *could* lead to clumpiness in the mass distribution with mass scales $M_{DW} \sim 3 \times 10^9\, M_\odot$ or $M_{BD} \sim 1.8 \times 10^8\, M_\odot$ respectively.

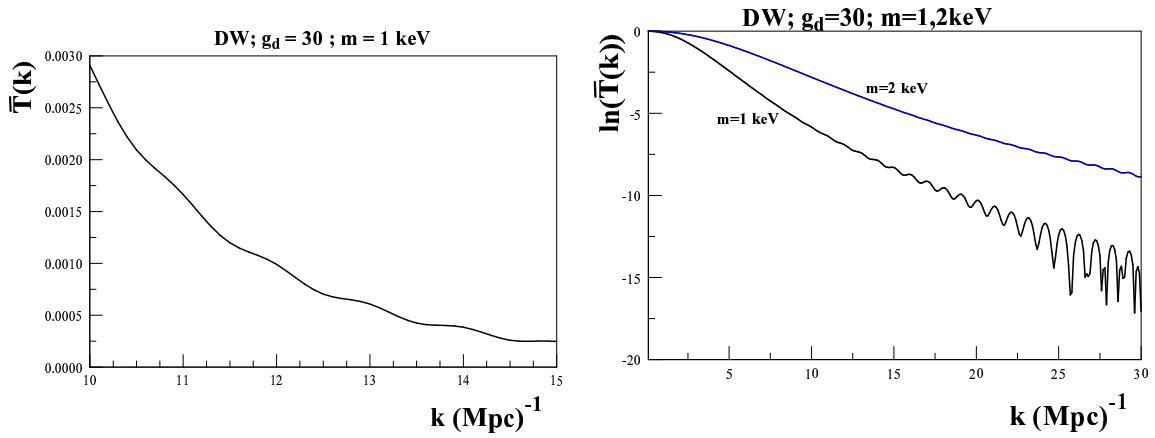

FIG. 7: Acoustic oscillations at small scales: (DW) species.

The smaller amplitudes of acoustic oscillations for the (BD) species as compared to the (DW) case is consistent with the fact that (BD) sterile neutrinos are *colder* and feature smaller velocity dispersions.

D. Power spectra: interpolation between large and small scales.

The power spectra normalized to CDM is given by

$$\overline{P}(k) = \left[\overline{T}(k)\right]^2, \tag{VI.50}$$

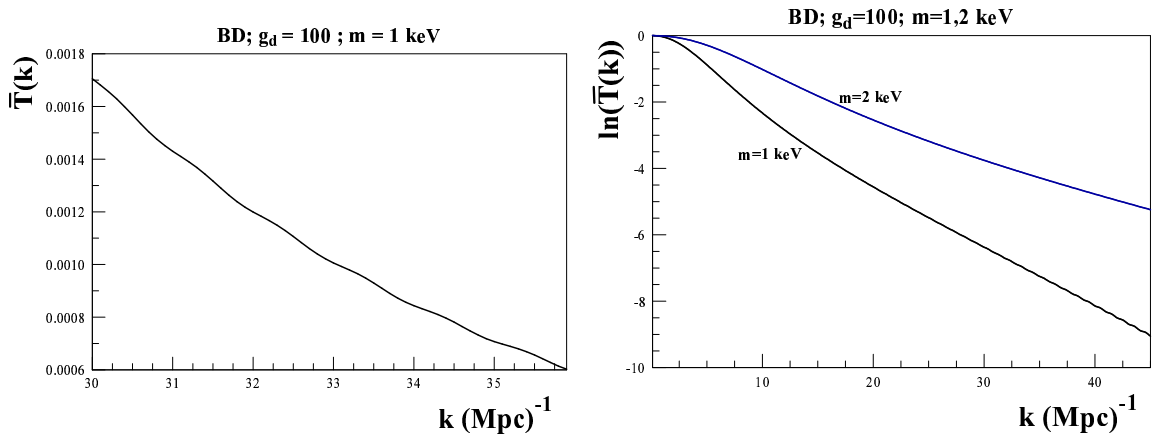

FIG. 8: Acoustic oscillations at small scales: (BD) species.

and the full power spectra is therefore,

$$P(k) = P_{CDM}(k)\,\overline{P}(k)\,. \tag{VI.51}$$

Since the transfer function for WDM particles is indistinguishable from that of CDM for small k, and as we have pointed out above the result (V.25) coincides within a few percent with the result by Bardeen et. al.[87]for $k \gg k_{eq}$, we use the numerical fit provided by Bardeen *et.al.*[87] for the CDM transfer function (without baryons) to extrapolate $P_{CDM}(k)$ to large scales:

$$P_{CDM}(k) = A\,k^{n_s}\left[T_{BBKS}(k)\right]^2 \tag{VI.52}$$

where A is the overall amplitude and is determined by the power spectrum of scalar fluctuations during inflation[76], and $n_s \simeq 0.96$ is the index of scalar perturbations during inflation[73]. Without baryons and with three relativistic (standard model) neutrinos [87]:

$$T_{BBKS}(k) = \frac{\ln\left[1+2.34\,q\right]}{2.34\,q}\left[1+3.89\,q+(16.1\,q)^2+(5.46\,q)^3+(6.71\,q)^4\right]^{-\frac{1}{4}}\;;\; q = \frac{k}{\Omega_m\,h^2}(\mathrm{Mpc})^{-1}\,. \tag{VI.53}$$

Combining eqns. (VI.50,VI.51,VI.52) and using the Born approximation for $\overline{T}(k)$ we find the following expression for the power spectra that interpolates between large and small scales,

$$P(k) = A\,k^{n_s}\left[\frac{4\,T_{BBKS}(k)}{(1+\kappa^2)(4+\kappa^2)}\,\frac{\int_{u_{eq}}^{0} Q(\kappa,u')\,\tilde{a}(u')\widetilde{I}[k;\kappa;u']\,du'}{\int_{u_{eq}}^{0} Q_2(u')\,\tilde{a}(u')\widetilde{I}^{CDM}[k;u']\,du'}\right]^2 \tag{VI.54}$$

The inhomogeneities $\widetilde{I}, \widetilde{I}^{CDM}$ are given by (VI.42-VI.48), $u_{eq} = -0.881$ and the mode functions Q_2, Q are given by eqns. (V.18,VI.27) respectively. The appendix gives a simplification of these terms along with a numerical implementation. This compact expression provides an interpolation between large and small scales that describes accurately the CDM limit for long-wavelengths $k \ll k_{fs}$ and captures the free streaming suppression at small scales encoded in the Born approximation. Its numerical implementation is fairly straightforward for arbitrary distribution functions, mass and decoupling temperature.

This is one of our main results.

E. Comparison to numerical results from Boltzmann codes:

The (WDM) power spectrum for non-thermal sterile neutrinos produced via the (DW) mechanism has been studied in refs.[32, 39–42]. The most recent studies using the Boltzmann codes CMBFAST[66] and or CAMB[67] have been reported in refs.[32, 41, 42]. The results of ref.[42] coincide with those of ref.[32] and are summarized by the fit given by eqns. (6,7) in ref.[32]. In both refs.[32, 42] the distribution function for sterile neutrinos is that given by eqn. (III.7) obtained in ref.[38]. However, the fitting function eqn. (6,7) given in ref.[32] (which reproduces the results of ref.[42]) fits the results of the Boltzmann code in the range $k < 5\ h\ \mathrm{Mpc}^{-1}$[32].

In ref.[41] the kinetic equation for production of sterile neutrinos given in ref.[38] was solved numerically and the solution was input in the numerical Boltzmann codes. In this reference the explicit form of the distribution function is not provided but instead a fitting formula for the transfer function normalized to CDM is given, eqn. (11,12) in this reference. Whereas both fitting functions in refs.[32, 41] are of the same *form*, they differ in the powers of momenta: at large k the fitting formula (11) in ref.[41] falls off with a power $\simeq k^{-6.93}$ whereas the fit given by eqn. (6) in ref.[32] falls of with a power $\simeq k^{-10}$. Therefore at small scales there is a large difference between these fits, whereas at large and intermediate scales there is a substantial agreement (see fig.4 in ref.[41]). Because in ref.[41] the distribution function has been obtained directly from the numerical integration of the kinetic equation derived in ref.[38], it is not clear whether the main differences with the results of ref.[32] are a consequence of the distribution function obtained numerically and input in the Boltzmann code being *different* from the form (III.7) which is the one used in refs.[32, 42].

Because our study relies on a pre-determined form of the distribution function and we neglect baryons, we can most directly compare our results with the distribution function (III.7) to the results in ref.[32], which also uses the form (III.7) and neglects baryons, however it includes $\Omega_\Lambda = 0.7$ which our study does not.

We compare our results for the transfer function $\overline{T}(k)$ (normalized to CDM) given by (VI.38) with those obtained from the fit given by eqns. (6,7) (for the non-thermal case) in ref.[32], with the caveat that this fit may *not* be the correct description of the power spectrum for $k > 5\ h\ \mathrm{Mpc}^{-1}$ as suggested by the discussion in ref.[32]. We also compare to the fit (11,12) in ref.[41], although this may *not* be fair comparison because we *assume* the distribution function (III.7) whereas in ref.[41] the effective distribution function may be different and the difference cannot be quantified in absence of a functional form. Furthermore, we use the "standard" value $g_d = 10.75$ for the comparison, whereas as discussed in ref.[41] the actual value may differ because this species of sterile neutrinos is produced very near the QCD phase transition where the effective number of relativistic degrees of freedom vary rapidly. Recognizing all these caveats we present the comparison of the transfer functions normalized to CDM in the range of masses and scales displayed in refs.[32, 41] in fig. (9), $m = 0.5, 1.0, 1.7\,\mathrm{keV}$: the solid line is $\overline{T}(k)$ from the Born approximation (VI.38), the dashed line is the fit given by eqns(6,7) for the non-thermal case in ref.[32], the dotted line is the fit (11,12) in ref.[41].

We find a remarkable agreement, to less than 5% with the fit given by eqns. (6,7) (non-thermal case) in ref.[32] in a wide range in which their fit is valid (see discussion in ref.[32]) for $m \gtrsim 1\,\mathrm{keV}$ the agreement is substantially better in a far larger range. In fig. (9) the comparison is in the range displayed in refs.[32, 41] to highlight agreements and discrepancies. In all cases reported in the literature the range studied or displayed are for wavectors k *far smaller* than the range in which the acoustic oscillations become manifest. The *approximate* estimate (VI.49) for the threshold suggests that for $m = 0.5, 1.0, 1.7$ keV oscillations should be manifest for $k \gtrsim 5.4, 10.8, 18.5\ (\mathrm{Mpc})^{-1}$ (corresponding to $k \gtrsim 7.5, 15.0, 25.6\ h\ (\mathrm{Mpc})^{-1}$ respectively). Fig. (10) displays $\overline{T}(k)$ from (VI.38) in a linear-linear scale for $k \gtrsim 2k_{fs}$ for $m = 1.0, 1.7$ keV. These figures are the continuation of the *same* $\overline{T}(k)$ displayed as solid lines in fig. (9) to the smaller scales $k \gtrsim 2k_{fs}$ in each case.

This comparison, with all the caveats mentioned above, suggests that the semi-analytic formulation along with the Born approximation summarized by (VI.38) captures the essential

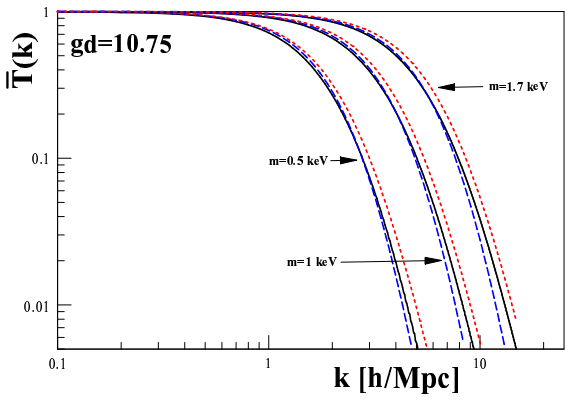

FIG. 9: Comparison of the transfer function for DW with $g_d = 10.75$ normalized to CDM with the results from Boltzmann codes. The solid line is the semi-analytic result from eqn. (VI.38), the (blue) dashed line is the result from the interpolation eqns.(6,7) (non-thermal case) from ref.([32]), the (red) dotted line is the result from the interpolating fit eqn. (11,12) in ref. ([41]). For all cases $h = 0.72, \Omega_{DM}h^2 = 0.133, g_d = 10.75$.

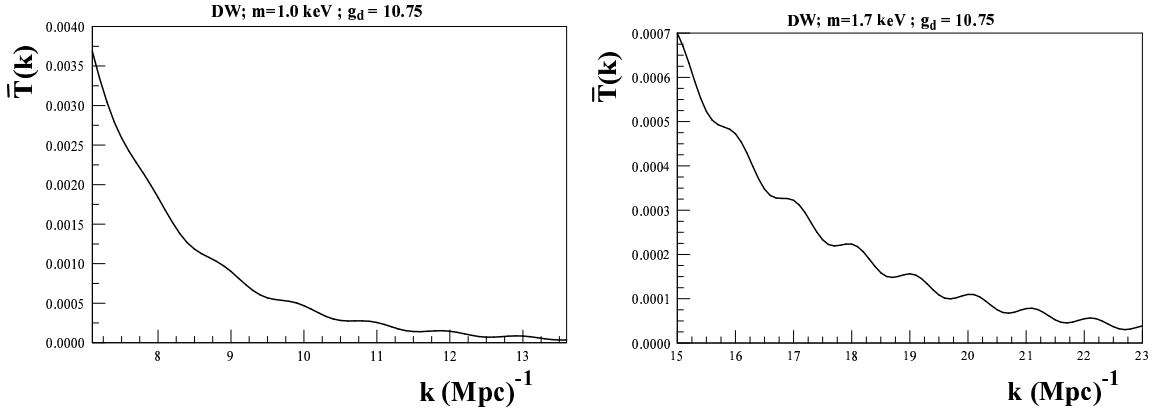

FIG. 10: $\overline{T}(k)$ from the semianalytic approximation (VI.38) displaying the acoustic oscillations at small scales $k \gtrsim 2k_{fs} \sim 10.8, 18.5$ $(\mathrm{Mpc})^{-1}$ for $m = 1.0, 1.7\mathrm{keV}$ respectively. Note that the horizontal scale is in $(\mathrm{Mpc})^{-1}$ and that vertical scales differ by a factor 5 between the two figures.

physical processes and provide a reliable tool to study the transfer function and power spectra for arbitrary distribution functions.

F. Applications:

Having established a direct comparison between the semi-analytic method and the results from Boltzmann codes in refs.[32, 41] and having confirmed the reliability of the method for the case of (DW) sterile neutrinos, we now compare the results for the case of (BD) production mechanism, which as mentioned above yields a highly non-thermal distribution function which is similar to that obtained from inflaton[43] and gravitino[62] decay.

The (DW) distribution function is proportional to a thermal distribution function and the proportionality constant *only* determines the abundance but is irrelevant for the free streaming length or indeed the transfer function (as can be gleaned from the previous sections).

There is a quasi-degeneracy between the (DW) and (BD) power spectra for different masses: a more massive WDM particle with a (DW) distribution function features a similar power spectrum as a less massive one but with a (BD) distribution function in a wide range of scales. This is explicitly shown in fig. (11) which displays the power spectra normalized to CDM (VI.50).

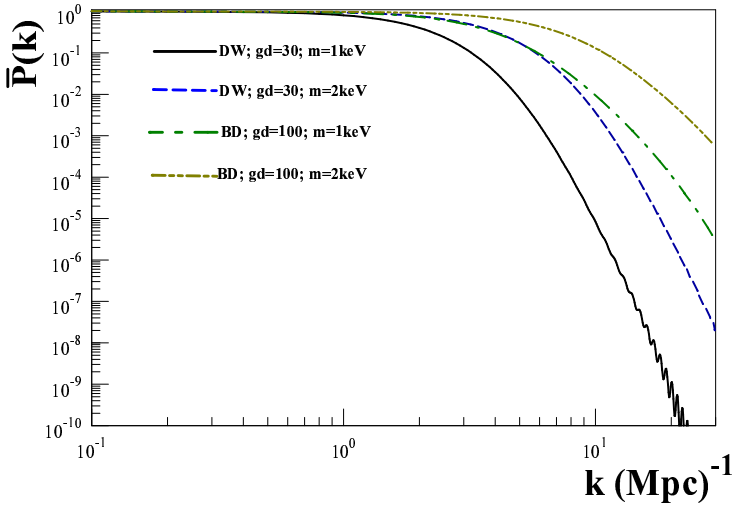

FIG. 11: The power spectra normalized to CDM for DW and BD with $m = 1, 2\,\mathrm{keV}$. Note that for the same mass the BD (colder species) is less suppressed than the DW (hotter species).

From this figure it is clear that $\overline{P}(k)$ for (DW) with $m = 2\,\mathrm{keV}$ is almost indistinguishable from $\overline{P}(k)$ for (BD) with $m = 1\,\mathrm{keV}$ for $k \lesssim 6 - 8\,(\mathrm{Mpc})^{-1}$. This is because the (BD) sterile

neutrinos are *colder* for two reasons: they decouple earlier and their distribution function favors small momenta, therefore the (BD) WDM particle has *smaller* velocity dispersion. This quasi-degeneracy is not unexpected, the mass is *not* the only relevant indicator for the power spectrum of the WDM particle, but also two other important aspects must enter in the assessment: the decoupling temperature (the higher, the colder the particle) and the details of the distribution function at small momenta: enhanced small momentum behavior leads to a *colder species* and a less suppressed power spectrum, for a given mass.

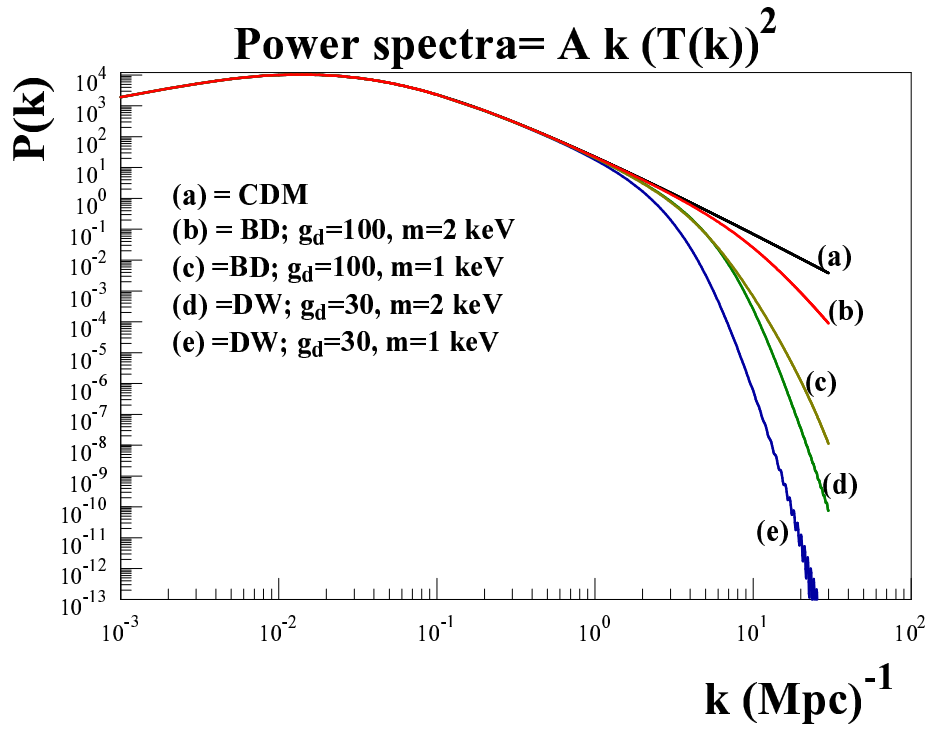

FIG. 12: The matter power spectra: $P(k) = A\,k\,(T(k))^2$ for $n_s = 1$ (A is the normalization amplitude) for CDM, DW and BD for $m = 1, 2$keV. Note the quasi degeneracy for DW with $m = 2$keV (d) and BD with $m = 1$keV (c) in a large range of $k \lesssim 12\,(\mathrm{Mpc})^{-1}$.

The full power spectra obtained using the interpolating eqn. (VI.54) for the two species considered here are shown in Fig. (12) which displays $P(k)$ for $n_s = 1\,;\,\Omega_m\,h^2 = 0.134$. Note how the two cases (c) (BD, $m = 1\,\mathrm{keV}$) and (d) (DW, $m = 2\,\mathrm{keV}$) are nearly indistinguishable for $k \lesssim 6 - 8\,(\mathrm{Mpc})^{-1}$.

VII. CONCLUSIONS AND DISCUSSIONS

Our main result is a semi-analytic derivation of the evolution equations for WDM perturbations and their solutions at small scales in a radiation-matter cosmology for arbitrary mass and distribution function of the decoupled WDM particle, and a simple numerical implementation that yields the power spectra at small scales.

There are three stages in the evolution of density perturbations of WDM candidates that decouple while they are relativistic: stages I) and II) describe the evolution during the RD era when the particle is relativistic and non-relativistic respectively but the gravitational potential is dominated by the radiation fluid, during stage III, the particle is non-relativistic and matter density perturbations dominate the gravitational potential. We consider adiabatic initial conditions determined when all the cosmologically relevant modes are superhorizon. The collisionless Boltzmann equation is solved in the three stages by using the solution at the end of a stage as the initial condition for the next stage. The free streaming wavevector

$$k_{fs} = \frac{\sqrt{3}\, k_{eq}}{2\, \langle V_{eq}^2 \rangle^{\frac{1}{2}}}$$

where $\langle V_{eq}^2 \rangle^{\frac{1}{2}}$ is the mean square root velocity dispersion of the WDM particle at *matter-radiation equality* not only determines the scale of suppression but also determines the size of the comoving horizon when the WDM particle becomes non-relativistic:

$$\eta_{NR} = \frac{\sqrt{3}}{\sqrt{2}\, k_{fs}} \, .$$

During stages I) and II) the acoustic oscillations in the radiation fluid dominate the gravitational potential, leading to an ISW effect that amplifies WDM density perturbations on scales larger than the sound horizon at η_{NR}. This amplification translates in a prolonged plateau in the transfer function for $k \lesssim k_{fs}$ which is more pronounced for *colder* species since these feature a larger k_{fs}.

When the particle is non-relativistic and WDM perturbations dominate the gravitational potential, the evolution is described by the Boltzmann-Poisson equation which yields an integral equation for density perturbations and is equivalent to integro-differential equation with an inhomogeneity and initial conditions determined by the past history during stages I and II. This equation is amenable to a systematic Fredholm expansion valid at small scales, whose leading order is the Born approximation which establishes a direct relation with a

fluid description of WDM perturbations. The resulting fluid equation is the generalization of Meszaros' equation for CDM but with an inhomogeneity and initial conditions that incorporate suppression by free streaming during the first two stages. The Born approximation lends itself to a simple numerical implementation for *arbitrary distribution functions and mass of the decoupled WDM particle*. Its main ingredients are the growing and decaying solution of the generalized Meszaros fluid equation for WDM perturbations, and the initial conditions and inhomogeneity that are completely determined by the past history during the first two stages. The solutions of the fluid equations feature *(WDM)-acoustic oscillations* which are manifest in the transfer function and power spectra for $k \gtrsim 2k_{fs}$.

An approximate form of the power spectra that interpolates between large and small scales for arbitrary distribution functions is given by eqn. (VI.54) and a simple and concise summary of the main elements of the Born approximation and its numerical implementation are provided in the appendix.

As an application of the method and its numerical implementation we study in detail and compare the transfer functions and power spectra of sterile neutrinos with mass in the $\sim$ keV range for two non-resonant production mechanisms: Dodelson-Widrow (DW) (sterile-active mixing) and Boson-decay (BD) near the electroweak scale. The former yields a distribution function proportional to a thermal fermion but with a decoupling temperature $T_d \sim 150\,\mathrm{MeV}$, whereas the latter leads to a strongly non-thermal distribution with a decoupling temperature $T_d \sim 100\,\mathrm{GeV}$ that favors small momentum and yields a *colder* species of sterile neutrinos for a given mass. For a sterile neutrino with mass $\sim$ keV the (DW)-species is *warmer* with $k_{fs}^{(DW)} \simeq 7.7\,(\mathrm{Mpc})^{-1}$ and the (BD)-species is *colder* with $k_{fs}^{(BD)} \simeq 14.12\,(\mathrm{Mpc})^{-1}$ and its transfer function features a longer plateau for $k \lesssim k_{fs}$ as a consequence of the ISW enhancement during stage I.

The study of the (DW) species allows us to directly compare the results for the transfer function from the semi-analytic formulation presented here to the results obtained in refs.[32, 41, 42] from the Boltzmann codes. Although we recognized several caveats in the comparison, we find excellent agreement to $< 5\%$ between the results from the Born approximation (VI.38) and the numerical fit to the result of Boltzmann codes presented in ref.[32] in the region of scales where the fit is valid. Thus while this WDM scenario may already be ruled out by Lyman-α constraints the detailed comparison between the method presented here and the results from Boltzmann codes confirm the reliability of our results.

Although the power spectra is strongly suppressed by free streaming at the scales at which (WDM) acoustic oscillations emerge, we *conjecture* that non-linear gravitational collapse *may* amplify these oscillations into peaks and troughs in the matter distribution at small scales, leading to clumpiness on mass scales associated with these scales, for example for a $m \sim$ keV sterile neutrino produced via the (BD) mechanism this scale is about $\sim 10^8 M_\odot$. Perhaps coincidentally this is of the order of the mass contained within a *half-light radius* in the (DM) halos of spiral, low surface brightness and dwarf spheroidal galaxies[88].

Having established the reliability of the method with a benchmark case, the next step of the program will implement these methods to obtain the power spectra for sterile neutrinos with different distribution functions obtained from the different production mechanisms. The method and its numerical implementation is quite general, independently of the particular WDM candidate and reliably yields the transfer function normalized to CDM for any WDM species that freezes out and becomes non-relativistic during the radiation dominated era.

A numerical solution of the full Gilbert equation (VI.3) along with its comparison to the Born approximation will be reported elsewhere.

Acknowledgments

DB and JW are supported by NSF grant award PHY-0852497. JW thanks support through Daniels and Mellon Fellowships.

Appendix A: Simplification of I_1

It is convenient to introduce the variables

$$x = \frac{k\eta}{\sqrt{3}} \quad ; \quad \varpi(k) = \frac{4\sqrt{2}}{\sqrt{3}} \frac{k}{k_{eq}} \gg 1 \tag{A.1}$$

and change integration variable from u' to η using eqns. (III.32,II.8)), yielding

$$I_1 = -6 I_a \tag{A.2}$$

$$I_a = \frac{1}{\alpha y} \int_{x_{NR}}^{x_{eq}} f(x) \frac{d}{dx}\Big(\frac{\sin(x)}{x}\Big) \sin\Big[\alpha\, y\big(U - \frac{1}{2}\ln(x) + \frac{1}{2}\ln[f(x)]\big)\Big] dx \tag{A.3}$$

where

$$U = u + \frac{1}{2}\ln[\varpi(k)] \quad ; \quad f(x) = 1 + \frac{x}{\varpi(k)} \tag{A.4}$$

$$x_{eq} = \frac{k\,\eta_{eq}}{\sqrt{3}} \simeq 69.3\,k\,(\mathrm{Mpc}) \;\; ; \;\; x_{NR} = \frac{\kappa}{2\sqrt{3}} \tag{A.5}$$

Integrating by parts and neglecting terms $\propto 1/\varpi(k) \ll 1$ we find

$$\begin{aligned} I_a \;&=\; \frac{1}{2}\big[1+\sqrt{2}\big]\frac{\sin(x_{eq})}{x_{eq}\alpha\,y}\sin\Big[\alpha\,y\big(u+0.787\big)\Big] \\ &-\; \frac{\sin(x_{NR})}{x_{NR}\alpha\,y}\sin\Big[\alpha\,y\Big(u-\frac{1}{2}\ln\Big(\frac{\langle V^2_{eq}\rangle^{\frac{1}{2}}}{4}\Big)\Big)\Big] \\ &+\; \frac{1}{2}\int_{x_{NR}}^{x_{eq}}\frac{\sin(x)}{x^2}\,\cos\Big[\alpha\,y\big(U-\frac{1}{2}\ln(x)\big)\Big]dx\,. \end{aligned} \tag{A.6}$$

In the second and third line in the above expression we have approximated $f(x) \sim 1$ since $x_{NR}/\varpi(k) \sim \langle V^2_{eq}\rangle^{\frac{1}{2}} \ll 1$ and the contribution from the upper limit to the integral in the third line (the region where $x/\varpi(k) \sim 1$) is suppressed by $\sim 1/x^2_{eq} \sim k^2_{eq}/k^2$. It is convenient to extract the singular term $\propto 1/x$ as $x \sim x_{NR}$ when $x_{NR} \ll 1$ (this is the CDM limit), integrating by parts again, leading to

$$\begin{aligned} I_a \;&=\; \frac{1}{2}\big[1+\sqrt{2}\big]\,\frac{\sin(x_{eq})}{x_{eq}\,\alpha\,y}\sin\Big[\alpha\,y\big(u+0.787\big)\Big] - \frac{\sin\big[\alpha\,y\,U\big]}{\alpha\,y} \\ &+\; \Big[1-\frac{\sin(x_{NR})}{x_{NR}}\Big]\frac{1}{\alpha\,y}\,\sin\Big[\alpha\,y\Big(u-\frac{1}{2}\ln\Big(\frac{\langle V^2_{eq}\rangle^{\frac{1}{2}}}{4}\Big)\Big)\Big] \\ &+\; \frac{1}{2}\int_1^{x_{eq}}\frac{\sin(x)}{x^2}\,\cos\Big[\alpha\,y\big(U-\frac{1}{2}\ln(x)\big)\Big]dx \\ &-\; \frac{1}{2}\int_1^{x_{NR}}\frac{[\sin(x)-x]}{x^2}\,\cos\Big[\alpha\,y\big(U-\frac{1}{2}\ln(x)\big)\Big]dx \end{aligned} \tag{A.7}$$

The CDM limit corresponds to $\alpha \to 0, x_{NR} \to 0$

Appendix B: Numerical implementation of the Born approximation.

The first step in the numerical implementation is to obtain $\sqrt{\overline{y}^2}$ for the given distribution function of decoupled WDM particles and to input this value into the mode functions Q, P given by eqns. (VI.26-VI.29).

For numerical implementation, it is convenient to take the wavevector k in units of $(\mathrm{Mpc})^{-1}$ and to write

$$\alpha \;=\; c_1\,k \;\; ; \;\; c_1 = 0.22\left(\frac{2}{g_d}\right)^{\frac{1}{3}}\left(\frac{\mathrm{keV}}{m}\right) \tag{B.1}$$

$$\kappa \;=\; c_2\,k \;\; ; \;\; c_2 = c_1\sqrt{\overline{y}^2} \tag{B.2}$$

$$c_{22} \;=\; \frac{c_2}{2\sqrt{3}} = 0.289\,c_2 \tag{B.3}$$

along with eqns. (III.29,III.47)), lead to

$$
\begin{aligned}
I_1[k;y;u] = \quad & -6\Bigg\{ \frac{1}{c_1\,k\,y}\Big[1-\frac{\sin(c_{22}k)}{c_{22}k}\Big]\,\sin\Big[c_1\,k\,y\Big(u-\frac{1}{2}\ln\Big(\frac{\langle V_{eq}^2\rangle^{\frac{1}{2}}}{4}\Big)\Big)\Big] \\
& + \frac{0.017}{k^2\,c_1\,y}\,\sin[69.3\,k]\,\sin\Big[c_1\,k\,y\big(u+0.787\big)\Big] - \frac{\sin\big[c_1\,k\,y\,\big(u+2.904+0.5\ln(k)\big)\big]}{c_1\,k\,y} \\
& + \frac{1}{2}\int_1^{69.3\,k}\frac{\sin(x)}{x^2}\,\cos\Big[c_1\,y\big(u+2.904+0.5\ln(k)-0.5\ln(x)\big)\Big]dx \\
& - \frac{1}{2}\int_1^{c_{22}\,k}\frac{[\sin(x)-x]}{x^2}\,\cos\Big[c_1\,y\big(u+2.904+0.5\ln(k)-0.5\ln(x)\big)\Big]dx\Bigg\}
\end{aligned}
\tag{B.4}
$$

$$
\begin{aligned}
I_1^{CDM}[k;u] = \quad & -6\Bigg\{\frac{0.017}{k}\,\sin[69.3\,k]\big(u+0.787\big)\big) - \big(u+2.904+0.5\ln(k)\big) \\
& + \quad 0.211 - \frac{1}{2}\int_{69.3\,k}^{\infty}\frac{\sin(x)}{x^2}\,dx\Bigg\}
\end{aligned}
\tag{B.5}
$$

The last integral term is $\lesssim 10^{-3}$ for $k \geq 0.2$ and can be neglected for small scales.

$$
I_2[k;y;u] = -\frac{1}{2}\left(\frac{d\,\ln f_0(y)}{d\ln y}\right) j_0\Big[c_1\,k\,y\,(u-u_{NR})+0.5\,c_2\,k\Big] \tag{B.6}
$$

$$
I_2^{CDM}[k;u] = -\frac{1}{2}\left(\frac{d\,\ln f_0(y)}{d\ln y}\right) \tag{B.7}
$$

$$
I_{ISW}[k;y;u] = \frac{12}{c_2\,k}\int_0^1\frac{dt}{t^2}\left[\cos\big(c_{22}\,k\,t\big)-\frac{\sin\big(c_{22}\,k\,t\big)}{\big(c_{22}\,k\,t\big)}\right] j_1\Big[c_1\,k\,y(u-u_{NR})+0.5\,c_2(1-t)\Big] \tag{B.8}
$$

$$
I_{ISW}^{CDM} = 0 \tag{B.9}
$$

---

[1] See for example, J. Primack, New Astron.Rev. **49**, 25 (2005); arXiv:astro-ph/0609541; in *Formation of structure in the Universe* (Ed. A. Dekel, J. P. Ostriker, Cambridge Univ. Press, Cambridge, 1999) and references therein.

[2] B. Moore *et. al.*, Astrophys. J. Lett. **524**, L19 (1999).

[3] G. Kauffman, S. D. M. White, B. Guiderdoni, Mon. Not. Roy. Astron. Soc. **264**, 201 (1993).

[4] S. Ghigna *et.al.* Astrophys.J. **544**,616 (2000).

[5] A. Klypin *et. al.* Astrophys. J. **523**, 32 (1999); Astrophys. J. **522**, 82 (1999).

[6] B. Willman *et.al.* Mon. Not. Roy. Astron. Soc. *353*, 639 (2004).

[7] J. F. Navarro, C. S. Frenk, S. White, Mon. Not. R. Astron. Soc. **462**, 563 (1996).

[8] J. Dubinski, R. Carlberg, Astrophys.J. **378**, 496 (1991).

[9] J. S. Bullock *et.al.*, Mon.Not.Roy.Astron.Soc. **321**, 559 (2001); A. R. Zentner, J. S. Bullock, Phys. Rev. **D66**, 043003 (2002); Astrophys. J. **598**, 49 (2003).

[10] J. Diemand *et.al.* Mon.Not.Roy.Astron.Soc. **364**, 665 (2005).

[11] J. J. Dalcanton, C. J. Hogan, Astrophys. J. **561**, 35 (2001).

[12] F. C. van den Bosch, R. A. Swaters, Mon. Not. Roy. Astron. Soc. **325**, 1017 (2001).

[13] R. A.Swaters, *et.al.*, Astrophys. J. **583**, 732 (2003).

[14] R. F.G. Wyse and G. Gilmore, arXiv:0708.1492; G. Gilmore *et. al.* arXiv:astro-ph/0703308; G. Gilmore *et.al.* arXiv:0804.1919 (astro-ph); G. Gilmore, arXiv:astro-ph/0703370.

[15] G.Gentile *et.al* Astrophys. J. Lett. **634**, L145 (2005); G. Gentile *et.al.*, Mon. Not. Roy. Astron. Soc. **351**, 903 (2004); V.G. J. De Blok *et.al.* Mon. Not. Roy. Astron. Soc. **340**, 657 (2003), G. Gentile *et.al.*,arXiv:astro-ph/0701550; P. Salucci, A. Sinibaldi, Astron. Astrophys. **323**, 1 (1997).

[16] G. Battaglia *et.al.* arXiv:0802.4220.

[17] W. J. G. de Blok, arXiv:0910.3538.

[18] P. Salucci et al. MNRAS **378**, 41 (2007); P. Salucci, arXiv:0707.4370.

[19] R. Wojtak *et.al.* arXiv:0802.0429.

[20] M.K. Ryan Joung *et.al.*ApJ **692** L1 (2009).

[21] J. R. Primack, arXiv:0909.2247.

[22] B. Moore, *et.al.* Mon. Not. Roy. Astron. Soc. **310**, 1147 (1999);

[23] P. Bode, J. P. Ostriker, N. Turok, Astrophys. J **556**, 93 (2001)

[24] V. Avila-Reese *et.al.* Astrophys. J. **559**, 516 (2001).

[25] S.F. Shandarin, A.G. Doroshkevich, Ya.B. Zeldovich, Sov.Phys.Usp. **26** 46 (1983).

[26] J. R. Bond, G. Efstathiou, J. Silk, Phys. Rev. Lett. **45**, 1980 (1980).

[27] A. V. Tikhonov, A. Klypin,MNRAS **395**,1915 (2009).

[28] A. V. Tikhonov, S. Gottlober, G. Yepes, Y. Hoffman, arXiv:0904.0175.

[29] A. V. Maccio, F. Fontanot, arXiv:0910.2460.

[30] U. Seljak *et.al.* Phys. Rev. Lett. **97**, 191303 (2006); M. Viel *et.al.* Phys. Rev. Lett. **97** 071301 (2006).

[31] M. Viel *et. al.* , Phys.Rev.Lett. 100 (2008) 041304; A. Boyarsky *et.al.*, JCAP **05**, 012 (2009).

[32] M. Viel, *et. al.* Phys. Rev. **D71**, 063534 (2005).

[33] K. Abazajian, S. M. Koushiappas, Phys. Rev. **D74**, 023527 (2006).

[34] A. V. Maccio, M. Miranda, MNRAS **382**, 1225 (2007).

[35] T. Sawala *et.al*, arXiv:1003.0671.

[36] H. J. de Vega, N. Sanchez, Mon. Not. R. Astron. Soc. **404**, 885 (2010); arXiv:0907.0006 .

[37] H. J. de Vega, P. Salucci, N. G. Sanchez, arXiv:1004.1908 .

[38] S. Dodelson, L. M. Widrow, Phys. Rev. Lett. **72**, 17 (1994).

[39] S. Colombi, S. Dodelson, L. M. Widrow, Astrophys. J. **458**, 1 (1996).

[40] X. Shi, G. M. Fuller, Phys. Rev. Lett. **82**, 2832 (1999); K. Abazajian, G. M. Fuller, M. Patel, Phys. Rev. **D64**, 023501 (2001); K. Abazajian, G. M. Fuller, Phys. Rev. **D66**, 023526, (2002); G. M. Fuller *et. al.*, Phys.Rev. **D68**, 103002 (2003).

[41] K. Abazajian, Phys. Rev. **D73**,063506 (2006).

[42] S. H. Hansen *et. al.* Mon. Not. R. Astron. Soc. **333**, 544 (2002).

[43] M. Shaposhnikov, I. Tkachev, Phys. Lett. **B639**,414 (2006).

[44] A. Kusenko, arXiv:hep-ph/0703116; Int.J.Mod.Phys.**D16**,2325 (2008); T. Asaka, M. Shaposhnikov, A. Kusenko; Phys.Lett. **B638**, 401 (2006); P. L. Biermann, A. Kusenko, Phys. Rev. Lett. **96**, 091301 (2006).

[45] A. Kusenko, Phys.Rept.**481**, 1 (2009).

[46] A. Boyarsky, O. Ruchayskiy, M. Shaposhnikov, Ann.Rev.Nucl.Part.Sci.**59**, 191 (2009).

[47] A. Kusenko, Phys. Rev. Lett. **97**, 241301 (2006).

[48] K. Petraki, A. Kusenko, Phys. Rev. **D 77**, 065014 (2008).

[49] K. Petraki, Phys. Rev. **D 77**, 105004 (2008).

[50] M. Kaphinghat, Phys.Rev. **D72**, 063510 (2005).

[51] K. Jedamzik, M.Lemoine, G. Moultaka, JCAP **0607** 010 (2006).

[52] A. Boyarsky *et.al.* Mon. Not. Roy. Astron. Soc. **370**, 213 (2006); Phys. Rev. **D74**, 103506 (2006); A. Boyarski *et. al.* AA, **471**, 51 (2007); Astropart. Phys. **28**, 303 (2007); C. R. Watson

et. al. Phys. Rev. **D74**, 033009 (2006).

[53] M. Lowenstein, A. Kusenko, Astrophys.J.**714**,652 (2010); Astrophys.J **714** , 652 (2010); M. Loewenstein, A. Kusenko, P. L. Biermann; Astrophys.J.**700**, 426 (2009).

[54] A. Boyarsky *et.al.* arXiv:1001.0644.

[55] A. Palazzo, D. Cumberbatch, A. Slosar, J. Silk, Phys.Rev.**D76**, 103511 (2007); D. Cumberbatch, J. Silk, AIPConf.Proc.**957**,375 (2007),arXiv:0709.0279.

[56] S. Ando, A. Kusenko, Phys. Rev. D 81, 113006 (2010); I. M. Shoemaker, K. Petraki, A. Kusenko, arXiv:1006.5458

[57] D. Boyanovsky, Phys.Rev.**D78**, 103505 (2008).

[58] J. Wu, C.-M.Ho, D. Boyanovsky, Phys. Rev. **D80**, 103511 (2009).

[59] C. J. Hogan, J. J. Dalcanton, Phys. Rev. **D62**, 063511 (2000).

[60] D. Boyanovsky, H. J. de Vega, N. Sanchez, Phys. Rev. **D 77**, 043518 (2008).

[61] D. Boyanovsky, H. J. de Vega, N. Sanchez, Phys. Rev. **D 78**, 063546 (2008).

[62] D. Gorbunov, A. Khmelnitsky, V. Rubakov, JHEP **0812**, 055 (2008).

[63] J. R. Bond, A. S. Szalay, Astrophys. J. **274**, 443 (1983).

[64] E. W. Kolb, M. S. Turner, *The Early Universe* , (Addison-Wesley, Redwood City, CA) (1990).

[65] D. Boyanovsky, Phys. Rev. **D 77**, 023528 (2008).

[66] U. Seljak, M. Zaldarriaga, ApJ, **469**, 437 (1996); M. Zaldarriaga, U. Seljak, E. Bertschinger, ApJ, **494**, 491 (1998); M. Zaldarriaga, U. Seljak, ApJS **129**, 431 (2000). See http://www.cmbfast.org ; http://lambda.gsfc.nasa.gov

[67] A. Lewis, A. Challinor, Phys.Rev. **D66** 023531 (2002). See the CAMB page http://camb.info/.

[68] M. Doran, JCAP **0510**, 011 (2005); M. Doran, C. M. Mueller, JCAP **0409** , 003 (2004). See the CMBEASY page: http://www.thphys.uni-heidelberg.de/ robbers/cmbeasy/index.html.

[69] P. Meszaros, Astr.Astroph. , **37**,225 (1974)

[70] E. J. Groth, P. J. E. Peebles, Astr.Astroph. , **41**,143 (1975).

[71] P. J. E. Peebles, *The large scale structure of the Universe*, (Princeton series in Physics, Princeton Univ. Press, Princeton, 1980).

[72] M. Shoji, E. Komatsu, Phys. Rev. **D81**, 123516 (2010).

[73] E. Komatsu *et. al.* (WMAP collaboration), arXiv:1001.4538; D. Larson *et.al.* (WMAP collaboration), arXiv:1001.4635.

[74] A. Loeb, M. Zaldarriaga, Phys. Rev. **D71**, 103520 (2005).

[75] C.-P. Ma, E. Bertschinger, Astrophys. J. **455**, 7 (1995).

[76] S. Dodelson *Modern Cosmology*, (Academic Press, N.Y. 2003).

[77] M. Giovannini, *A Primer on the physics of the cosmic microwave background*, (World Scientific, Singapore, 2008).

[78] D. H. Lyth, A. R. Liddle, *The primordial density perturbation* (Cambridge University Press, Cambridge, UK, 2009).

[79] S. Weinberg *Cosmology*, (Oxford University Press, Oxford, 2008).

[80] R. Durrer, *The cosmic microwave background*, (Cambridge University Press, Cambridge, UK 2008).

[81] H. Kodama, M. Sasaki, Int. J. Mod. Phys.**A1**,265 (1986).

[82] E. W. Kolb, M. S. Turner, *The Early Universe* , Addison-Wesley, (1990).

[83] I. H. Gilbert, Astrophys. J. **144**, 233 (1966); **152**, 1043 (1968).

[84] E. Bertschinger, in *Cosmology and Large Scale Structure*, proceedings, Les Houches Summer School, Session LX, ed. R. Shaeffer *et. al.* (Elsevier, Amsterdam), 273 (1996), arXiv:astro-ph/9503125.

[85] S. Weinberg, Astrophys.J **581**, 810 (2002).

[86] W. Hu, N. Sugiyama, Astrophys. J. **471**, 542 (1996).

[87] J. Bardeen *et.al.* Astrophys. J. **304**, 15 (1986).

[88] M. Walker *et.al.*, arXiv:1004.5228; M. Walker *et.al.* arXiv:0906.0341.